

1 **We would like to thank the two anonymous referees and B. Bohn for their helpful comments and**
2 **suggestions. We have addressed all of these and outlined proposed updates we will make to the**
3 **manuscript in red below (comments in black):**

4
5 The authors used measured $j(\text{O}_1\text{D})$ photolysis frequencies as a model input. The $j(\text{O}_1\text{D})$
6 measurements were made with a filter radiometer on a 22 m tower and were covering downward
7 radiation from the upper hemisphere. In fact, because of low ground albedos upward radiation from
8 vegetated surfaces can usually be neglected in the UV-B range, at least for ground based
9 measurements. The same applies for the tower measurements at Mt. Schmücke in good
10 approximation. However, if the tower is situated into a cloud, upward radiation will increase
11 dependent on cloud optical thickness and tower height. In a very thick cloud the radiation field can
12 become virtually isotropic with up-welling radiation as strong as down-welling. Because of the
13 limited tower height this was probably not the case here, but nevertheless $j(\text{O}_1\text{D})$ could have been
14 significantly enhanced.

15 To estimate the potential contribution of upward radiation, simulations with the TUV model (also
16 used by the authors) were consulted for the Mt. Schmücke station on 01 Oct 2010 (mid of the
17 campaign period). Spectral actinic flux densities were calculated assuming a range of solar zenith
18 angles (SZA), a typical ozone column of 300 DU, standard aerosol, a ground albedo of 0.02, and an
19 elevation of 937 m. Model output was generated for 959 m representing the tower top at 22 m
20 above ground. Moreover, a homogeneous cloud cover of 1000 m thickness was assumed starting
21 directly at the ground and extending to about 2 km cloud top elevation which is typical for
22 continental stratus clouds. The total cloud optical depth (COD) was varied and from the simulated
23 spectra photolysis frequencies $j(\text{O}_1\text{D})$ were calculated.

24 In a first step the ratios of downward $j(\text{O}_1\text{D})$ under overcast and clear sky conditions was calculated
25 as a function of COD as shown in Fig. 1. These calculations reveal a non-linear dependence that can
26 be utilized to estimate the COD encountered during the campaign: a reduction by 70% as found
27 experimentally corresponds to a COD of about 30-40. These CODs are in reasonable agreement with
28 those that can be estimated from the liquid water content (LWC) measured at the tower top (Petty,
29 2006):

$$30 \quad \text{COD} = \frac{3L}{2\rho_l r_{\text{eff}}}$$

31 Here L is the liquid water path, ($L = \text{LWC} \times 1000 \text{ m}$), ρ_l is the density of liquid water and r_{eff} is the
32 effective cloud droplet radius which was assumed to be $10 \mu\text{m}$. LWCs between 0.1 and 0.3 g m^{-3} that
33 were measured at the tower result in CODs between 15 and 45.

34 In a second step the ratio total/downward $j(\text{O}_1\text{D})$ was calculated as shown in Fig. 2. Here a nonlinear
35 increase is observed. For the COD estimated above the enhancement factor is about 1.2.
36 Consequently, when the tower is in clouds the measured $j(\text{O}_1\text{D})$ should be scaled up accordingly. The
37 same applies for $j(\text{HCHO})$.

38
39 **We thank B. Bohn for his valuable comment and recommendations for estimating the upwelling**
40 **radiation present during cloud events which, in the original manuscript, we did not consider. We**
41 **have scaled the in-cloud measured $j(\text{O}_1\text{D})$ presented in figures 2 and 3 and the in-cloud $j(\text{O}_1\text{D})$ and**
42 **$j(\text{HCHO})$ used in the analytical expression to determine the first order loss of HO_2 to cloud droplets**
43 **as suggested. We find, on average, the photolysis rates are enhanced by approximately 17% during**
44 **cloud events when upwelling is considered. This in turn means that the first order loss process**
45 **required to reproduce in-cloud HO_2 observations increases modestly from 0.1 s^{-1} to 0.14 s^{-1} on**
46 **average. Owing to the fact that only minor changes in the first order loss are necessary, we still**
47 **observe good agreement for the HO_2 uptake coefficient calculated by varying the first order loss in**
48 **the analytical expression to reproduce HO_2 observations as a function of cloud water pH and the**
49 **theoretical expression derived by Thornton et al. suggesting that this theoretical expression remains**

1 appropriate to estimate the loss of HO₂ to cloud droplets even when enhancements in radiation are
2 included. All figures and discussions in the revised manuscript will be updated to account for in-
3 cloud enhancements of radiation and we will explicitly reference B. Bohn's comment and include an
4 outline of the methodology for estimating the contribution from upward radiation in the revised
5 manuscript.
6

7 1) As pointed out in the comment by B. Bohn, it is not clear whether the authors have taken upward
8 scattering of radiation when the tower was inside a cloud into account in their analytical expression
9 calculating HO₂ concentrations. As stated in the manuscript and illustrated in Figure 1, the FAGE cell
10 was oriented horizontal to the ground to prevent pooling of water on top of the inlet that could
11 enter the detection chamber. On page 23771, the authors state that j(O₁D) was measured "from the
12 top of the 22m tower, alongside the FAGE detection cell, using a 2_ filter radiometer." It is not clear
13 whether the radiometer was placed on top of the tower near the FAGE inlet but pointed upwards to
14 measure downward radiation, or placed alongside the horizontally oriented FAGE inlet. This should
15 be clarified in the revised manuscript.
16

17 The filter radiometer pointed upwards throughout the campaign and so only measured downward
18 radiation. It was located next to the FAGE inlet on the tower. We will clarify this in the revised
19 manuscript along with the corrections we have now made to account for upwelling radiation (please
20 see our response to B. Bohn's comment also).
21

22 2) The authors state that the FAGE instrument was calibrated twice weekly during the measurement
23 campaign in addition to calibrations before and afterwards. However, it is not clear that the
24 calibrations were done under conditions that attempt to simulate the water conditions inside the
25 cloud. How did the authors correct their data for quenching by water vapor during the in cloud
26 measurements? During HOxComp, it was found that there may have been an unknown factor
27 related to water vapor that may have influenced the HO₂ instrument sensitivities or may have
28 caused an unknown interference inside the FAGE cells (Fuchs et al., Atmos. Chem. Phys., 10, 12233–
29 12250, 2010). The authors should comment on the potential impact of water on their in-cloud
30 measurements of HO₂.
31

32 Calibrations were performed at relevant water vapour concentrations so as to encompass the
33 ambient water vapour concentrations observed. As such, no correction for quenching of the
34 fluorescence signal by water vapour is necessary and has not been made. In the lab we have studied
35 the impact of H₂O (v) on the sensitivity of this FAGE cell type (as outlined by Commane et al. ACP, 10,
36 8783-8801, 2010) by systematically varying the H₂O from 500 ppmV to 10 000 ppmV and observe
37 only ~ 10 % reduction in sensitivity over this H₂O range for both OH and HO₂ which can be entirely
38 explained by the known quenching of fluorescence by H₂O molecules. We will make a remark
39 reflecting this in the revised manuscript.
40
41

42 3) Incorporating HO₂ uptake onto cloud droplets into the GEOS Chem model leads to significant
43 changes in radical and H₂O₂ concentrations depending on the fate of aqueous HO₂. Figure 10 shows
44 that HO₂ uptake leading to the formation of water reduces surface radical and H₂O₂ concentration
45 (Figure 10a), while HO₂ uptake leading to the formation of H₂O₂ leads to an increase in surface H₂O₂
46 and less of a reduction in radical concentrations (Figure 10b). However, the column radical and H₂O₂
47 concentration changes appear to show the opposite when HO₂ uptake is incorporated into the
48 model (Figure 11). In this Figure HO₂ uptake leading to the formation of water leads to an increase in
49 the column H₂O₂ concentrations and less of a reduction in radical concentration (Figure 11a), while
50 HO₂ uptake leading to H₂O₂ formation leads to a decrease in the column H₂O₂ and a greater
51 reduction in the column radical concentrations (Figure 11b). On page 23778 the authors state

1 referring to the concentration of OH that “changes to the column values are only significant in the
2 case where H₂O₂ is not produced.” However, in Figure 11a (HO₂ uptake leading to water) the column
3 values of OH do not show a significant reduction, while a significant reduction in column OH is
4 shown in Figure 11b (H₂O₂ produced). Are the results in Figure 11a and b reversed?
5 The authors should clarify their discussion of these model results.

6
7 **Regrettably, we have labelled Figure 11 incorrectly and as spotted by the referee Figure 11 a)
8 actually represents the annually averaged fractional change in column HO₂, OH and H₂O₂ with the
9 inclusion of HO₂ uptake to clouds leading to the production of H₂O₂, whilst b) represents the column
10 change with the production of H₂O. We will correct the figure caption in the revised manuscript.**

11
12 Title: Seems a bit too broad for the actual content of the paper and could be more specific to include
13 a direct mention of observations in cloud.

14
15 **We propose ‘The influence of clouds on radical concentrations: Observations of OH and HO₂ during
16 the Hill Cap Cloud Thüringer (HCCT) campaign in 2010’ as an alternative title.**

17 Introduction: I do not see the classic paper by Jacob on cloud chemistry. Jacob, D. J. (1986),
18 Chemistry of OH in remote clouds and its role in the production of formic-acid and
19 peroxymonosulfate, *J. Geophys. Res.*, 91(D9), 9807–9826.

20
21 **This is an oversight, we will refer to the results from this classic paper on cloud chemistry in the
22 introduction of the revised manuscript.**

23
24 p 23776 end and 23777 beginning: The comparison of derived gamma values for uptake to cloud
25 droplets with laboratory measurements on aerosol particles is somewhat of an apples/oranges
26 problem. The aerosol particles probed in the lab will have very different ionic contents at the very
27 least, and possibly phase (depending on the experimental conditions). That they agree well or not
28 with values derived in cloud is therefore somewhat inconsequential.

29
30 **We agree that we are not comparing like with like. However, as no laboratory studies have been
31 performed which look at the uptake of HO₂ to cloud droplets, we feel this is the closest comparison
32 we can make. Many of the lab studies have been performed on aqueous aerosol. We will narrow the
33 comparison down to laboratory measured uptakes observed on aqueous aerosol in the revised
34 manuscript.**

35
36 p 23778, line 16. I think the value of gamma = 0.2 in GEOS-Chem goes back at least to Martin, R. V.,
37 D. J. Jacob, R. M. Yantosca, M. Chin, and P. Ginoux (2003), Global and regional decreases in
38 tropospheric oxidants from photochemical effects of aerosols, *J. Geophys. Res.*, 108(D3), 4097,
39 doi:10.1029/2002JD002622.

40
41 **The value of the gamma for HO₂ onto aerosol in the standard version of GEOS-Chem has some
42 history. The model has used the Thornton et al., parameterization in the past, and very high values
43 derived by Mao et al. 2013 (Mao, J., S. Fan, D.J. Jacob, K.R. Travis, *Radical loss in the atmosphere
44 from Cu-Fe redox coupling in aerosols, Atmos. Chem. Phys.*, 13,509-519, 2013b.) Given the
45 uncertainties in the value of the gamma the Model Steering Committee now considers a uniform
46 value of 0.2 to offer the advantage of simplicity. Thus we have returned to the Martin et al value but
47 via a path which has taken us through Thornton and Mao. We will include this reference for the
48 gamma value used in GEOS-Chem in the revised manuscript.**

49
50 Figure 4 - is the data in this figure a compilation of many different cloud events, or is it one cloud
51 event where the surface area might be correlated with time and

1
2 This data is a compilation of all daytime cloud events. We will update the text to clarify this.
3
4 pg 23778, line 11, missing a reference after "Thornton".

5 This will be included.

6 1. I'm quite surprised there is such a large effect upon "surface" HO₂ due to clouds, especially large
7 in the mid and higher latitudes. Are these results the effects of HO₂ uptake to both aerosol and
8 cloud relative to no uptake, or really just the effect of uptake to cloud only, on top of an uptake to
9 aerosol at $\gamma = 0.2$? These results should be compared to those from Thornton et al 2008,
10 McIntyre and Evans, Martin et al 003, etc focused upon the effect of HO₂ uptake to aerosol particles.
11 Aerosol particles are more likely distributed throughout the vertical near the surface than cloud
12 (outside of fog situations anyway), and the impacts of having fast uptake of HO₂ to aerosol particles
13 were comparable to those reported here.

14 The plots do show the difference between simulations with HO₂ uptake onto clouds and those
15 without. We note that the magnitude of the changes calculated here are generally consistent with
16 the simulations presented in (Huijnen et al., 2014, Atmos. Chem. Phys. Discuss., 14, 8575–8632,
17 2014 www.atmos-chem-phys-discuss.net/14/8575/2014/ doi:10.5194/acpd-14-8575-2014) although
18 the figures in Huijnen et al are not directly comparable with our plots. We now include a plot of the
19 liquid water mass concentrations in the model both as a zonal mean and column integrated in the
20 publication to show that in the GEOS-5 met fields there is significant liquid water in the lowest most
21 levels of the model leading to the uptake.

22 2. The question is for such a short lived species like HO_x, how do cloud, presumably located at the
23 top of the boundary layer or higher, affect surface HO₂ concentrations? Does HO₂ loss in cloud
24 become a major sink of boundary layer O₃ in the model, and therefore impacts the HO_x production
25 outside of cloud? Liang and Jacob JGR 1997 found little impact of cloud chemistry on ozone over N.
26 America, which seems somewhat consistent with the results presented here. In fact, Liang and
27 Jacob mention the impact of cloud chemistry on ozone might be significant in stratus capped marine
28 boundary layer regions. It would be helpful to therefore show the perturbation to modeled surface
29 O₃ due to incorporating HO₂ uptake in cloud in the model. I assume this output from the model
30 already exists and new simulations would not be needed.

31 We now include plots of the impact on O₃ concentrations in our figures. The impact on O₃ is minor
32 globally as the regions where HO₂ is perturbed the most are the regions where the HO₂ lifetime is
33 long as the NO concentration is low. Thus the impact over ozone production areas is minimal and
34 the impact on O₃ destruction is small. Impacts are highest where there are clouds over low NO_x area.

35 3. How were the cloud fields in GEOS-Chem prescribed? Were they fixed between simulations of
36 uptake/no uptake so as to represent the exact same radiation fields and vertical distributions, etc?
37 Does GEOS-Chem realistically represent air mass transport through cloud and thus the average time
38 air spends within cloud?

1 The model prescribes the cloud liquid water in each grid box from the GEOS-5 Meteorological
2 analysis. Thus the impact of clouds on the radiation field and the vertical distribution of the clouds
3 will be identical in all simulations. The model representation of cloud processes is by necessity of the
4 grid resolution (~250km) fairly crude. However other studies which need to invoke cloud chemistry
5 within the model (notably for SO₂ oxidation) suggest that the model is capable of reproducing these
6 features with some fidelity (see for example Alexander, B., D.J. Allman, H.M. Amos, T.D. Fairlie, J.
7 Dachs, D.A. Hegg and R.S. Sletten, Isotopic constraints on sulfate aerosol formation pathways in the
8 marine boundary layer of the subtropical northeast Atlantic Ocean, J. Geophys. Res., 117, D06304,
9 doi:10.1029/2011JD016773, 2012).

10 4) This section should be expanded to address the above, and also include a discussion on the
11 impact of HO₂ uptake in cloud upon the tropospheric ozone burden.

12 We now include such a discussion.

13

14 **The influence of clouds on radical concentrations:**
15 **Observations and modelling studies of HO_x during the Hill**
16 **Cap Cloud Thüringia (HCCT) campaign in 2010**

Formatted: Font: Arial, 16 pt, Bold,
Font color: Auto

17 **L. K. Whalley^{1,2}, D. Stone², I. J. George^{2,*}, S. Mertes³, D. van Pinxteren³, A.**
18 **Tilgner³, H. Herrmann³, M. J. Evans^{4,5} and D.E. Heard^{1,2}**

Deleted: Influence of clouds on the
oxidising capacity of the
troposphere

19 [1] {National Centre for Atmospheric Science, University of Leeds, Leeds, LS2 9JT, UK}

20 [2] {School of Chemistry, University of Leeds, Leeds, LS2 9JT, UK}

21 [3] {Leibniz-Institut für Troposphärenforschung (TROPOS), Permoserstr. 15, 04318 Leipzig, Germany}

22 [4] {National Centre for Atmospheric Science, University of York, York, YO10 5DD, UK}

23 [5] {Department of Chemistry, University of York, York, YO10 5DD, UK}

24 [*] {Now at National Risk Management Research Laboratory, U.S. Environmental Protection Agency,
25 Research Triangle Park, North Carolina 27711, USA}

26 Correspondence to: L. K. Whalley (l.k.whalley@leeds.ac.uk)

27

28 **Abstract**

1 The potential for chemistry occurring in cloud droplets to impact atmospheric composition
2 has been known for some time. However, the lack of direct observations and uncertainty in
3 the magnitude of these reactions, led to this area being overlooked in most chemistry
4 transport models. Here we present observations from Mt. Schmücke, Germany, of the HO₂
5 radical made alongside a suite of cloud measurements. HO₂ concentrations were depleted in-
6 cloud by up to 90% with the rate of heterogeneous loss of HO₂ to clouds necessary to bring
7 model and measurements into agreement demonstrating a dependence on droplet surface area
8 and pH. This provides the first observationally derived assessment for the uptake coefficient
9 of HO₂ to cloud droplets and was found to be in good agreement with theoretically derived
10 parameterisations. Global model simulations, including this cloud uptake, showed impacts on
11 the oxidizing capacity of the troposphere that depended critically on whether the HO₂ uptake
12 leads to production of H₂O₂ or H₂O.

13

14 1 Introduction

15 Clouds occupy around 15% of the volume of the lower troposphere and can impact
16 atmospheric composition through changes in transport, photolysis, wet deposition and in-
17 cloud oxidation of sulphur. Modelling studies have shown that aqueous phase chemistry can
18 also significantly reduce gaseous HO₂ concentrations by heterogeneous uptake and loss into
19 cloud droplets (Jacob, 1996; Tilgner et al., 2005; Huijnen et al., 2014). This chemistry is
20 predicted to reduce OH and O₃ concentrations also due to the reduction in the gas-phase
21 concentration of HO₂. This in turn, decreases the self-cleansing capacity of the atmosphere
22 and increases the lifetime of many trace gases (Lelieveld and Crutzen, 1990) with impacts for
23 climate and air quality. Aqueous phase models have been developed which combine
24 multiphase chemistry with detailed microphysics (Tilgner et al., 2005), but there are limited
25 experimental field data of gas-phase radical concentrations within clouds to corroborate
26 model predictions of heterogeneous loss of radicals to cloud droplets. There have been a
27 number of aircraft campaigns which have measured OH and HO₂ radical concentrations
28 within clouds (Mauldin et al., 1997; Mauldin et al., 1998; Olson et al., 2004; Commane et al.,
29 2010), often, however, simultaneous observations of cloud droplet number and size
30 distributions (or other key gas-phase radical precursors) were not made during these studies,
31 making it difficult to assess the full impact of clouds on radical concentrations. In general
32 therefore climate and air quality models do not consider this impact of clouds on atmospheric
33 composition.

Deleted: (

Deleted: b

Deleted: b

1 Within the literature, a wide range of uptake coefficients of HO₂ to liquid and aerosol
2 surfaces have been considered to reproduce observed HO₂ concentrations (e.g. (Sommariva et
3 al., 2004; Haggerstone et al., 2005; Emmerson et al., 2007; Whalley et al., 2010)) with often
4 large uptake coefficients (up to 1 at times) used to reconcile model over-predictions. A wide
5 range of uptake coefficients, not wholly consistent with each other, have been reported from
6 laboratory studies (Abbatt et al., 2012). From measurements conducted in our laboratory,
7 uptake probabilities of HO₂ to sub-micron aerosols were found to be less than 0.02 at room
8 temperature (George et al., 2013) for aqueous aerosols that did not contain significant
9 transition metal ions; similarly low uptake coefficients were derived by Thornton and Abbatt
10 (2005). In contrast, measurements by Taketani et al. (2008) suggest higher uptakes of ~0.1
11 with enhancements observed with increasing relative humidity.

12

13 The uptake of HO₂ to aqueous aerosols is driven by its high solubility in water owing to its
14 high Henry's Law constant ($H_{\text{HO}_2} = 4.0 \times 10^3 \text{ M atm}^{-1}$ at 298.15 K (Hanson et al., 1992)).

15 Once in the aqueous phase, reaction between dissolved HO₂ and its conjugate base, O₂⁻,
16 occurs rapidly. Thornton et al. (2008) have demonstrated that the solubility and reactivity of
17 HO₂ is temperature and pH dependent and if the well characterised aqueous phase reactions
18 (Sect. 2.3, (R1) – (R5)) alone are representative of the heterogeneous loss processes, only
19 small uptake coefficients would be expected at room temperature, consistent with the work
20 by George et al. (2013) and Thornton and Abbatt (2005). The enhanced uptake coefficients
21 reported by Taketani et al. (2008) suggests that there may be additional competing
22 mechanisms occurring, however.

23

24 Further uncertainties arise in the literature relating to the eventual gas-phase products from
25 these aqueous-phase reactions. The general consensus, until recently, was that these reactions
26 would ultimately produce H₂O₂ (Jacob, 1996), but the significance of the reactions depends
27 critically on whether this is the case or whether, instead, H₂O is produced (Macintyre and
28 Evans, 2011). This is significant as H₂O₂ can photolyse to return odd hydrogen
29 (HO_x=OH+HO₂) to the gas phase, whilst cloud uptake of HO₂ to form H₂O provides a
30 terminal sink for HO_x. Recent work by Mao et al. (2013) postulates that a catalytic
31 mechanism involving the coupling of the transition metal ions Cu(I)/Cu(II) and Fe(II)/Fe(III)
32 may rapidly convert HO₂ to H₂O, rather than H₂O₂ in aqueous aerosols. The concentration
33 and availability of dissolved Fe and Cu in cloud droplets tends to be much lower than in

Deleted: .

1 aqueous aerosol (Jacob, 2000) with a large fraction of Cu ions present as organic complexes
2 (Spokes et al., 1996; Nimmo and Fones, 1997) which are far less reactive towards O_2^- and
3 $HO_2(aq)$ than the free ions (Jacob, 2000) and so it is uncertain whether the mechanism put
4 forward by Mao et al. (2013) could be extended to heterogeneous processes occurring within
5 cloud droplets.

6 To better understand the role of clouds and heterogeneous processes on the oxidative capacity
7 of the troposphere, coordinated gas-phase measurements of OH and HO_2 within clouds
8 together with aerosol-cloud microphysical measurements are needed. The Hill Cap Cloud
9 Thuringia 2010 (HCCT-2010) campaign which took place in 2010 aimed to characterise the
10 interaction of particulate matter and trace gases in orographic clouds. This paper presents the
11 impact of cloud droplets on measured gas-phase OH and HO_2 and uses these observations to
12 assess the proposed aqueous phase mechanisms and determine the global impact of clouds on
13 the tropospheric oxidising capacity.

14 **2 Experimental**

15 The HCCT-2010 campaign took place at the Thüringer Wald mountain range in central
16 Germany during September and October 2010. The radical measurements were made from
17 the German Weather Service (DWD) and the Federal Environmental Office (UBA) research
18 station located close to the summit of Mt. Schmücke (the highest peak in the mountain range,
19 937 m above sea level, $10^{\circ}46'8.5''$ East, $50^{\circ}39'16.5''$ North). In October, the UBA station is
20 immersed in cloud for 25 days on average (Herrmann et al., 2005) and, hence, is highly
21 suitable for the study of gas and aerosol interactions with orographic cloud. Two additional
22 experimental sites, approximately 4 km upwind of the summit site at Goldlauter and
23 approximately 3 km downwind of the summit at Gelhberg were also equipped with a number
24 of instruments which enabled the processing of a single air parcel as it passed through a cloud
25 to be assessed by multiphase trajectory models such as SPACCIM (SPectral Aerosol Cloud
26 Chemistry Interaction Model (Wolke et al., 2005); see Sect. 2.3). Further details of the
27 locations may be found in Herrmann et al. (2005).

28 **2.1 Radical measurements**

29 OH and HO_2 measurements were made using the fluorescence assay by gas expansion
30 technique (FAGE). Details of the instrumentation can be found in Whalley et al. (2010). A
31 single FAGE fluorescence cell was used for sequential measurements of OH and HO_2 . This

1 was operated from the top of a 22 m high tower to co-locate with cloud measurements and
2 ensure that the measurements were performed in full cloud. The cell was held at 1 Torr using
3 a roots blower backed rotary pump system which was housed in an air-conditioned shipping
4 container at the base of the tower (Fig. 1) and was connected to the cell via 30 m of flexible
5 hosing (5 cm OD). 308 nm tuneable, pulsed laser light was used to electronically excite OH
6 radicals, this was delivered to the cell via a 30 m fibre optic cable (Oz optics) with the laser
7 system (a Nd:YAG pumped Ti:Sapphire, Photonic Industries) housed in the shipping
8 container. Fluorescence was detected by a channel photo multiplier (CPM) (Perkin Elmer)
9 and gated photon counting. Data were acquired every second (photon counts from 5000 laser
10 shots), with a data acquisition cycle consisting of 220 seconds with the laser wavelength
11 tuned to the OH transition (NO was injected after 110 sec to rapidly convert HO₂ to OH, to
12 allow the quantification of HO₂) and 110 sec tuned away from the OH transition to determine
13 the background signal from laser scattered light.

14 The sensitivity of the fluorescence cell for OH and HO₂ was determined twice weekly during
15 the measurement period through calibration using VUV photolysis of H₂O vapour in a
16 turbulent flow of zero air (BOC, BTCA air). Calibrations were performed at relevant H₂O
17 vapour concentrations so as to encompass the ambient H₂O vapour concentrations observed.
18 As such, no correction for quenching of the fluorescence signal due to changing conditions
19 was necessary. The impact of H₂O (v) on the sensitivity of this FAGE cell type (as outlined
20 by Commane et al., (2010)) has been studied by systematically varying the H₂O
21 concentration from 500 ppmV to 10 000 ppmV and only ~ 10 % reduction in sensitivity over
22 this range for both OH and HO₂ was observed. This reduction is entirely explained by the
23 known quenching of fluorescence by H₂O molecules. The lamp flux was determined by N₂O
24 actinometry (see Commane et al. (2010) for further details); this was carried out before and
25 after the campaign and the values agreed within 21%; the average flux was used to determine
26 the sensitivity. The limit of detection (LOD) at a signal to noise ratio of one for one data
27 acquisition cycle was ~6×10⁵ molecule cm⁻³ and ~8.5×10⁵ molecule cm⁻³ for OH and HO₂,
28 respectively.

29 A number of operational modifications (from the standard University of Leeds ground-based
30 operations (Whalley et al., 2010)) were necessary to facilitate measurements of the gas-phase
31 concentrations of the radicals within clouds. As tower measurements were required
32 (schematic of the measurement set-up is provided in Fig. 1), a single, smaller (4.5 cm (ID)

Formatted: Font: (Default) Times New Roman, 12 pt, Font color: Auto

Formatted: Font: (Default) Times New Roman, 12 pt, Font color: Auto

Formatted: Font: (Default) Times New Roman, 12 pt, Font color: Auto

Formatted: Font: (Default) Times New Roman, 12 pt, Font color: Auto

Formatted: Font: (Default) Times New Roman, 12 pt, Font color: Auto

Formatted: Font: (Default) Times New Roman, 12 pt, Font color: Auto

Formatted: Font: (Default) Times New Roman, 12 pt, Font color: Auto

Formatted: Font: (Default) Times New Roman, 12 pt, Font color: Auto

Formatted: Font: (Default) Times New Roman, 12 pt, Font color: Auto

Formatted: Font: (Default) Times New Roman, 12 pt, Font color: Auto

Formatted: Font: (Default) Times New Roman, 12 pt, Font color: Auto

Formatted: Font: (Default) Times New Roman, 12 pt, Font color: Auto

Formatted: Font: (Default) Times New Roman, 12 pt, Font color: Auto

1 diameter stainless steel cylinder) FAGE fluorescence cell, based on the University of Leeds
2 aircraft cell design (Commane et al., 2010) was used for sequential measurements of OH and
3 HO₂. Ambient air was drawn into the cell through a 1 mm diameter pinhole nozzle. The
4 distance between sampling nozzle and radical detection region was 18 cm and NO (10
5 SCCM, BOC, 99.5%) was injected ~8 cm below the nozzle for titration of HO₂ to OH.

6 The fluorescence cell was orientated with the nozzle pointing horizontal to the ground in an
7 attempt to minimise water pooling on the nozzle and being sucked into the cell during cloud
8 events. Occasional droplets were ingested by the cell and resulted in an instantaneous large
9 increase in the laser scattered signal. These spiked increases were discreet and short-lived; the
10 data presented here have been filtered to remove these spikes, which were easy to identify.

11 Tests have been conducted post-campaign to determine the level of HO₂ interference from
12 RO₂ radicals (Fuchs et al., 2011). Under this particular experimental set-up, an equivalent
13 amount of ethene-derived RO₂ radicals to HO₂ were found to contribute 46 % to the total
14 HO₂ signal (Whalley et al., 2013). The FAGE instrument was found not to be sensitive to
15 CH₃O₂, and other short-chain alkane-derived RO₂ radicals but is sensitive to other alkene and
16 aromatic derived RO₂ radicals with similar sensitivities to that for ethene-derived RO₂. The
17 instrument is also sensitive to longer-chain alkane-derived RO₂ radicals (>C₃) albeit to a
18 smaller extent, as reported by Whalley et al. (2013). For this rural environment, at this time of
19 year, however, the contribution of alkene and aromatic-derived RO₂ radicals to the total RO₂
20 budget is expected to be small as the parent VOCs for these particular RO₂ types were at low
21 concentrations; isoprene concentrations, for example, were on average just 12.6 pptv. As a
22 consequence of this, the resultant HO₂ interference from RO₂ radicals should also be low.

23 **2.2 Model expression and constraints**

24 An analytical expression has been used to predict the mean diurnal HO₂ concentrations
25 throughout the campaign both during cloud events and outside of cloud events. This
26 expression was originally developed by Carslaw et al. (1999) for modelling OH, HO₂ and
27 RO₂ radicals in the marine boundary layer and was found to agree with full Master Chemical
28 Mechanism (MCM) model predictions for OH and HO₂ to within 20% for daytime hours. It
29 has since been extended further by Smith et al. (2006) to include additional HO₂ sinks, such
30 as heterogeneous loss (k_{Loss}). The expression, given in Eq. (3), derives from the solution of
31 simultaneous steady state expressions for OH and CH₃O₂ (Eq. (1) and Eq. (2) below) and

1 includes any primary sources of HO₂ not coming from radical propagation steps such as
 2 formaldehyde photolysis:

$$3 \quad [OH] = \frac{2f \cdot j(O^1D)[O_3] + [HO_2](k_{HO_2+NO}[NO] + k_{HO_2+O_3}[O_3])}{k_{CO+OH}[CO] + k_{H_2+OH}[H_2] + k_{HCHO+OH}[HCHO] + k_{CH_4+OH}[CH_4] + k_{NO_2+OH}[NO_2] + k_{O_3+OH}[O_3]} \quad (1)$$

$$4 \quad [CH_3O_2] = \frac{k_{CH_4+OH}[CH_4][OH]}{k_{CH_3O_2+HO_2}[HO_2] + k_{CH_3O_2+NO}[NO]} \quad (2)$$

5

$$6 \quad \beta[HO_2]^3 + \gamma[HO_2]^2 + \delta[HO_2] + \varepsilon = 0 \quad (3)$$

7 where

$$\beta = 2k_{T2}(k_{T3}B + k_{T1}A)$$

$$\gamma = 2k_{T3}k_{T2}J_1 + 2k_{T3}k_{P5}[NO]B + 2k_{T2}k_{P4}[CH_4]B + k_T[NO_2]k_{T2}B + 2Ak_{T1}k_{P5}[NO]$$

$$\delta = 2k_{T3}k_{P5}J_1[NO] + 2k_{T2}k_{P4}J_1[CH_4] + k_TJ_1[NO_2]k_{T2} + k_TB[NO_2]k_{P5}[NO] - (J_1 + J_2)Ak_{T2}$$

$$\varepsilon = J_1k_T[NO_2]k_{P5}[NO] - (J_1 + J_2)Ak_{P5}[NO]$$

8 where

$$J_1 = P(OH) = 2f[O_3]j(O^1D)$$

9 (*f* is the fraction of O(¹D) that reacts with H₂O vapour to form OH, rather than being
 10 quenched to O(³P))

$$J_2 = 2j(HCHO \rightarrow 2HO_2)[HCHO]$$

$$A = k_{CO+OH}[CO] + k_{H_2+OH}[H_2] + k_{HCHO+OH}[HCHO] + k_{CH_4+OH}[CH_4] + k_{NO_2+OH}[NO_2] + k_{O_3+OH}[O_3]$$

$$B = k_{HO_2+NO}[NO] + k_{HO_2+O_3}[O_3] + k_{loss}$$

$$k_T = k_{OH+NO_2}$$

$$k_{T1} = k_{HO_2+HO_2}$$

$$11 \quad k_{T2} = k_{HO_2+CH_3O_2}$$

$$12 \quad k_{T3} = k_{OH+HO_2}$$

1 $k_{P4} = k_{CH_4+OH}$

2 $k_{P5} = k_{CH_3O_2+NO}$

3 Limited CO concentration data are available from the summit site during the project, owing
4 to instrumental problems for the first two weeks of measurements. An average CO
5 concentration of 231 ppbv was used in the analytical expression to determine HO₂
6 concentrations although additional model runs at + and - 1σ of this average concentration
7 (297 ppbv and 165 ppbv respectively) were also made to assess the sensitivity of the
8 predicted HO₂ concentration to this constraint. Similarly, only discrete (non-continuous)
9 measurements of HCHO were made during the project; an average value of 479 pptv was
10 used as a model constraint and further model runs at + and - 1σ of this average concentration
11 (818 pptv and 139 pptv respectively) were made.

12 $j(O^1D)$ was measured from the top of the 22 m tower, alongside the FAGE detection cell,
13 using a 2-π filter radiometer (Bohn et al., 2008), which pointed skywards throughout the
14 campaign. The photolysis rates of formaldehyde, $j(HCHO)$, have been calculated using the
15 Tropospheric Ultraviolet and Visible (TUV) radiation model (Madronich and Flocke, 1998).
16 The correlation between TUV calculated $j(HCHO)$ with TUV calculated $j(O^1D)$ was
17 determined allowing these photolysis rates to be scaled to the measured $j(O^1D)$ values to
18 account for the presence of clouds. During cloud events, upward radiation will increase, with
19 the magnitude of this increase dependent on the cloud optical depth (COD) and measurement
20 height (Bohn, 2014). The contribution of upward radiation as a function of COD has been
21 estimated using the TUV model using the methodology outlined by Bohn (2014). This
22 estimated increase in upward radiation has been added to the in-cloud photolysis rates
23 presented in Section 3. On average, photolysis rates are enhanced by ~17% during cloud
24 events due to upwelling. A constant value of 1760 ppbv was assumed for CH₄ and a value of
25 508 ppbv was taken for H₂. O₃ and NO_x measurements were made from the top of the tower
26 using commercial analysers which ran continuously from the 16th September (day 3 of the
27 field project). Details of the ancillary measurements used for comparison and model
28 constraints are provided in Table 1. Further details of many of the measurement techniques
29 can be found in the overview paper from an earlier hill cap cloud experiment, the Field
30 Investigations of Budgets and Conversions of Particle Phase Organics in Tropospheric Cloud
31 Processes (FEBUKA) project (Herrmann et al., 2005).

Deleted: .

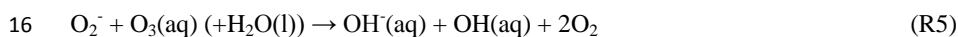
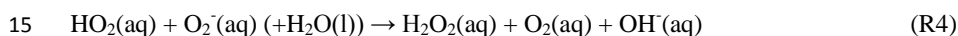
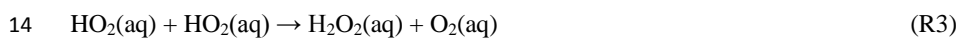
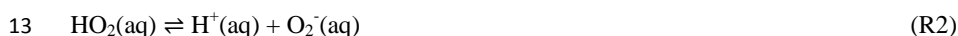
1 Rate coefficients are taken from the most recent recommendations in the Master Chemical
2 Mechanism (MCMv3.2), <http://mcm.leeds.ac.uk/MCM/>.

3 A constant uptake rate for HO₂ (k_{Loss}) of 0.14 s⁻¹ to cloud droplets was included during cloud
4 events to reproduce the average HO₂ in-cloud observations. Additional model runs with no
5 uptake during cloud events have also been run for comparison, as have model runs in which
6 the first order loss to droplets was varied to replicate the HO₂ observations as a function of i)
7 cloud droplet surface area and ii) pH (Sect. 3.1).

8

9 2.3 Aqueous phase chemistry

10 An outline of the aqueous phase reactions thought to be occurring, and which converts HO₂
11 to H₂O₂, is given below:



17 The equations used to calculate the theoretical increase in γ_{HO_2} with increasing pH, as
18 proposed by Thornton et al. (2008), which have been compared with γ_{HO_2} determined in this
19 work (Sect. 3.1), are given by:

$$20 \frac{1}{\gamma_{\text{HO}_2}} = \frac{1}{\alpha_{\text{HO}_2}} + \frac{3\omega N_A}{8000(H_{eff}RT)^2 k_{eff}[\text{HO}_2(\text{g})]r_P} \quad (4)$$

21 where

$$22 H_{eff} = H_{\text{HO}_2} \left[1 + \frac{K_{eq}}{[\text{H}^+]} \right] \quad (5)$$

23 and

Deleted: 1

$$k_{eff} = \frac{k_3 + \left(\frac{K_{eq}}{[H^+]_{aq}}\right)k_4}{\left(1 + \frac{K_{eq}}{[H^+]_{aq}}\right)^2} \quad (6)$$

The values used in Eq. (4) – Eq. (6) to calculate γ_{HO_2} are provided in Table 2.

2.4 Trajectory model

In addition to the modelling exercises, outlined in Sect. 2.2 above, an up-to-date chemistry process model, SPACCIM (SPectral Aerosol Cloud Chemistry Interaction Model (Wolke et al., 2005)) has been used to simulate the gas phase HO_2 radical concentrations along a trajectory during the mountain overflow of an air parcel passing an orographic hill cap cloud to further explore the heterogeneous loss processes occurring during the cloud events encountered. This model combines complex microphysical and detailed multiphase chemistry, permitting a detailed description of the chemical processing of gases, deliquesced particles and cloud droplets. SPACCIM incorporates the MCMv3.1-CAPRAMv4.0a mechanism (Master Chemical Mechanism (Saunders et al., 2003) / Chemical Aqueous Phase RADical Mechanism (Tilgner et al., 2013; Braeuer et al., in preparation)) with 11381 gas phase and 7125 aqueous phase reactions. The MCMv3.1-CAPRAM4.0a mechanism incorporates a detailed description of the inorganic and organic multiphase chemistry including phase transfer in deliquesced particles and cloud droplets based on a time-dependent size-resolved aerosol/cloud spectra. Further details about the SPACCIM model framework and the chemical mechanisms are given elsewhere in the literature (Tilgner et al., 2013; Wolke et al., 2005; Sehili et al., 2005) (and references therein).

The measured meteorological data as well as the physical and chemical aerosol and gas phase data at the upwind site in the village of Goldlauter provided the basis for the time-resolved initialisation of the model. In addition, separate initial box model runs with the MCM mechanism were performed to provide a more comprehensive initialisation of the chemical gas phase composition at the simulation start. SPACCIM simulations were performed with an air parcel advected along a predefined orography-following trajectory from the upwind site (Goldlauter) through the hill cap cloud, passing Mt. Schmücke (summit site), to the downwind site (Gehlberg). Parcel simulations were performed every 20 minutes allowing a time-resolved comparison of the predicted and measured HO_2 data at the summit site.

29

Deleted: CAPRAMv3.0n
Deleted: 3
Deleted: n
Formatted: Font: Times New Roman, 12 pt
Deleted: Braeuer
Deleted: 2013
Deleted:)
Formatted: Font: (Default) Times New Roman, 12 pt
Deleted: 777
Deleted: 77
Deleted: CAPRAM3.0n
Deleted: 3
Deleted: n

1 2.5 Global chemistry transport model

2 The GEOS-Chem model version 9.1.3 (www.geoschem.org) has been run to assess the global
3 impact of the uptake of HO₂ by cloud droplets. The model was run at 2x2.5 degree global
4 resolution for two years. The first year was considered a spin-up and has been ignored. The
5 standard model includes uptake of HO₂ onto aerosols (with an uptake coefficient of 0.2), but,
6 the model has been updated in this work to include an uptake of HO₂ onto clouds. This is
7 parameterized as a first order loss onto clouds in a similar way to that onto aerosols following
8 Schwartz (1984) using the temperature dependent parameterization of Thornton et al. (2008)
9 with a cloud pH of 5. The cloud surface area is derived from the cloud liquid water in the
10 each model grid box (provided from the meteorological analyses) and cloud droplet radius is
11 taken to be 6µm over continents and 10µm over oceans. Clouds below 258 K are assumed to
12 be ice and no uptake occurs. The parameterization takes diffusional limitation in the gas
13 phase into account but not in the cloud phase. All simulations use the same cloud liquid water
14 fields, thus the impact of clouds on photolysis, wet deposition and transport is identical in all
15 simulations.

16 3 Results and Discussion

17 Near continuous OH and HO₂ measurements were made at the Mt. Schmücke site from 13th
18 September to 19th October 2010, during which 35 separate orographic cloud events were
19 encountered which lasted as little as 24 min to more than 2 days in duration. Fig. 2 shows the
20 time-series of OH, HO₂, j(O¹D), NO, O₃ and liquid water content. OH concentrations were
21 close to or below the limit of detection (LOD) of the instrument for much of the measurement
22 period. A clear diurnal signal was only observable when several days of data were averaged
23 together outside of cloud events (Fig. 3). The peak OH concentration was observed at midday
24 at $\sim 1 \times 10^6$ molecule cm⁻³. No clear OH diurnal profile was observed during cloud events.
25 HO₂ concentrations were variable depending on whether the site was in cloud or not. The
26 average diurnal peak concentration of HO₂ was $\sim 4 \times 10^7$ molecule cm⁻³ outside of cloud
27 events (Fig. 3). A diurnal profile of HO₂ was also observed when sampling within clouds
28 with peak concentrations reduced by approximately 90% on average. The measured rate of
29 ozone photolysis, j(O¹D), varied with time of day and cloud thickness. Daily peak photolysis
30 rates were $8.8 \times 10^{-6} \text{ s}^{-1}$ and $4.1 \times 10^{-6} \text{ s}^{-1}$ outside and within clouds, respectively. Clouds thus
31 reduced photolysis rates by ~~60~~%.

Deleted: 3.6

Deleted: 7

1 Fig. 4 shows the dependence of measured HO₂ concentration on cloud droplet surface area
2 for all daytime cloud events. The observed HO₂ concentration has been divided by the
3 observed $j(O^1D)$ to remove the impact of the changing photolysis rates within the cloud. This
4 ratio has then been normalized to 1 when the droplet surface area was zero and plotted
5 against the cloud droplet surface area. The decrease in the ratio with increasing droplet
6 surface area suggests that in addition to the reduction in HO₂ caused by a reduction in the
7 photolysis rates within clouds, there is a further loss process of HO₂ that increases with cloud
8 droplet surface area. A similar decrease in the ratio is also observed with increasing liquid
9 water (not shown). From these observations it becomes apparent that a heterogeneous process
10 must be occurring in the presence of clouds.

11 An insight into the mechanism by which HO₂ is lost to clouds is demonstrated by the
12 dependence of the measured HO₂ concentration as a function of cloud water pH (Fig. 5a).
13 Throughout the project the pH of the cloud water was recorded every hour and ranged from
14 3.4 to 5.3. The lowest in-cloud HO₂ occurred in clouds with the highest cloud water pH
15 suggesting that the solubility of HO₂ was enhanced at higher pH as might be expected given
16 that HO₂ is a weak acid.

17 **3.1 Determining the uptake coefficient for HO₂ to cloud droplets**

18 The analytical expression derived by Carslaw et al.(1999), and given in Eq. (3), has been
19 used to estimate HO₂ concentrations both in and out of cloud events (Fig. 6). The expression
20 represents reasonably well the campaign mean diurnal observation of HO₂ outside of the
21 cloud events during the daytime (red dashed line and shading). During cloud events,
22 however, the model (black dashed line and shading) over-estimates the observed (grey line)
23 HO₂ throughout the day. The inclusion of a first order loss process ($k_{Loss}=0.14\text{ s}^{-1}$) in the
24 analytical expression is able to bring the observations and calculation into better agreement
25 on average. The cloud droplet surface area was variable during the different cloud events
26 encountered ($1.2\pm 0.4\times 10^3\text{ cm}^2\text{ m}^{-3}$) although no diurnal trend in this parameter was evident.
27 A clear anti-correlation between the observed HO₂ concentration and droplet surface area was
28 observed and this correlation could only be reproduced by the analytical expression by
29 increasing k_{Loss} in the model from $2.0\times 10^{-2}\text{ s}^{-1}$ to $3.5\times 10^{-1}\text{ s}^{-1}$ as the surface area increased
30 from $1.2\times 10^2\text{ cm}^2\text{ m}^{-3}$ to $1.5\times 10^3\text{ cm}^2\text{ m}^{-3}$ (Fig. 7).

Deleted: 1

Deleted: 1

Deleted: 4

Deleted: 2

1 This first order loss rate can be converted into an uptake coefficient (γ_{HO_2}) using Eq. (7)
2 (Schwartz, 1984). Using campaign mean values for cloud surface area (A) of $1.2 \times 10^3 \text{ cm}^2 \text{ m}^{-3}$,
3 droplet radius (r_p) of $6 \text{ }\mu\text{m}$, gas phase diffusion constant for HO_2 (D_g) of $0.25 \text{ cm}^2 \text{ s}^{-1}$, and
4 molecular speed of HO_2 (ω) of 64000 cm s^{-1} gives an uptake coefficient of 0.01; the uptake
5 coefficient as a function of cloud droplet surface area is presented in the upper panel of figure
6 7.

Deleted: 0065

Deleted: 065

$$7 \quad k_{loss} = \left(\frac{r_p}{D_g} + \frac{4}{\gamma_{HO_2} \omega} \right)^{-1} A \quad (7)$$

8 These derived uptake coefficients are in good agreement with laboratory studies (Abbatt et
9 al., 2012), including recent measurements in our laboratory, which ranged between 0.003 –
10 0.02, for heterogeneous loss of HO_2 on aqueous $(NH_4)_2SO_4$, $NaCl$ and NH_4NO_3 sub-micron
11 aerosols (George et al., 2013). This methodology provides, for the first time, a direct field
12 assessment of the heterogeneous rate of loss of HO_2 .

13 Repeating this analysis but splitting the observations by cloud pH leads to values of
14 γ_{HO_2} ranging from 1.65×10^{-3} at a pH of 3.7 to 8.84×10^{-2} at a pH of 5.2 (Fig. 5b). These values
15 are in good agreement with those calculated by Thornton et al. (2008) suggesting that the
16 Thornton mechanism (which is based entirely on the known aqueous phase chemistry) is in
17 play in real clouds and that it can be used to estimate the heterogeneous loss of HO_2 to cloud
18 surfaces in the troposphere.

Deleted: 1.04×10^7

Deleted: 1

Deleted: 0

Deleted: 1

19 SPACCIM simulations (Wolke et al., 2005) have also been carried out, focussing on one
20 particular cloud event which fulfilled the required meteorological and connected flow
21 conditions for the cloud passage experiment (additional simulations relating to the other
22 cloud events encountered during HCCT will be presented in future publications). The
23 modelled and measured HO_2 concentrations at Mt. Schmücke during the cloud event,
24 FCE1.1, are presented in Fig. 8. Comparisons between modelled and measured
25 concentrations demonstrate the simulated HO_2 concentrations are in a similar range as the
26 measurements. The mean simulated HO_2 concentrations of 3.1×10^6 molecule cm^{-3} for
27 FCE1.1 are a factor of 1.4 greater than the HO_2 measurements which were, on average
28 2.2×10^6 molecule cm^{-3} during this particular cloud event. A further trajectory model
29 simulation has been run and compared to measured HO_2 concentrations at Mt. Schmücke
30 during a non-cloud event, NCE0.8, also. Fig. 9 reveals that the model is able to reproduce the

Deleted: 0

1 modelled HO₂ concentrations well and tracks the temporal concentration profile throughout
2 this event. The mean predicted HO₂ concentration is just 24% smaller than the measurements.

3 The agreement between the trajectory modelled and measured in-cloud HO₂ values confirms
4 the significant reductions of radicals within clouds predicted by complex multiphase box
5 models in the past (Lelieveld and Crutzen, 1990; Tilgner et al., 2005; Tilgner et al., 2013) and
6 supports the findings presented above. Importantly, the results imply that the phase transfer
7 data for HO₂ used within SPACCIM simulations, e.g. the applied mass accommodation
8 coefficient ($\alpha_{HO_2} = 10^{-2}$), are appropriate to reproduce the reduced HO₂ concentrations for in-
9 cloud conditions. These applied parameters control the uptake fluxes towards the aqueous
10 phase and, ultimately, the aqueous phase HO_x levels. Confidence in the values assumed for
11 these parameters is essential to model in-cloud oxidation within the aqueous phase
12 accurately, with the multiphase chemistry of other important chemical subsystems, such as
13 the S(IV) to S(VI) conversion, the redox-cycling of transition metal ions and the processing
14 of organic compounds all heavily dependent upon the values taken.

15 3.2 Global impact of the uptake of HO₂ onto cloud droplets

16 The GEOS-Chem Chemistry Transport Model (www.geos-chem.org) has been used to assess
17 the impact of the uptake of HO₂ onto cloud droplets on the global oxidizing capacity using
18 the, now field-validated, mechanism of Thornton et al. (2008). To investigate both the impact
19 of the uptake and whether H₂O₂ is produced three simulations are run, i) with no cloud uptake
20 of HO₂, ii) with cloud uptake (assumed pH of 5) of HO₂ using the Thornton mechanism to
21 produce H₂O₂, and iii) with cloud uptake (assumed pH of 5) of HO₂ to produce H₂O. All
22 simulations include HO₂ uptake onto aerosol with γ_{HO_2} of 0.2, which is the standard value
23 used in GEOS-Chem (Martin et al., 2003; Macintyre and Evans, 2011).

24 Fig. 10 shows the annual fractional change in surface HO₂, OH, H₂O₂ and O₃ concentrations
25 with cloud uptake switched on, and with either H₂O₂ being produced or not. Column changes
26 are shown in Fig. 11. Both with and without H₂O₂ production, the impact is most evident in
27 areas with long HO₂ lifetimes, i.e. regions with low NO_x and low HO₂ concentrations, and
28 with significant cloud water densities (see Figure 12). These are concentrated in the extra-
29 tropics with up to 25% and 10% reduction in surface and column concentrations respectively.
30 The impact on the H₂O₂ concentration depends critically on whether H₂O₂ is produced or not
31 within clouds. In the extra-tropics there are up to 30% increases in surface H₂O₂ if it is

Deleted: a

Deleted: .

Deleted: (

Deleted:

Deleted: and

Formatted: Subscript

Deleted: .

Deleted:

1 produced with a similar reduction if it is not. The impact on surface extra-tropical oxidizing
2 capacity (OH) are of the order 10-20% for both cases, but changes to the column values are
3 only significant in the case where H₂O₂ is not produced. Changes in O₃ concentration are
4 surprisingly small in both simulations. This reflects both the anti-correlation between NO
5 concentrations and HO₂ lifetimes, and the low cloud water densities over the polluted
6 continental regions. The largest fractional changes in HO₂ concentration occur in regions
7 which are not producing O₃. The change in the lifetime due to the HO₂ uptake onto clouds
8 thus has little impact on O₃ production. The large surface impact of the cloud uptake
9 primarily reflects uptake of HO₂ by clouds at the surface (see figure 12a) rather than a
10 transported impact of cloud processes from aloft downwards. The small impact on O₃ is
11 consistent with results of Liang and Jacob, (1997). These simulations make a variety of
12 approximations (see Sect. 2.5) but they indicate that the uptake of HO₂ onto clouds at the
13 rates observed in this field campaign may offer a substantial perturbation to the oxidizing
14 capacity (OH and H₂O₂) of the atmosphere, especially in the extra-tropics, but seems to have
15 a very small impact on O₃ concentrations.

16 4 Conclusions

17 We have shown here experimentally for the first time that the uptake of HO₂ onto clouds can
18 have a significant impact on the composition of the atmosphere in a way consistent with
19 theoretical predictions. It seems likely, however, that chemistry occurring within clouds will
20 have other currently unknown impacts on the composition of the atmosphere. Global and
21 regional models need to be developed further to investigate these impacts with predictive pH
22 an especially important development. The impact of these processes may also change in the
23 future with climate induced impacts on the hydrological cycle. Further laboratory, field
24 studies and modelling are required to help resolve these remaining complex questions.

25 Acknowledgements

26 The authors would like to thank Dr. Trevor Ingham, John Spence and Matthew Broadbent for
27 help with the development of the FAGE instrument to facilitate tower measurements. HCCT-
28 2010 was partially funded by the German Research Foundation (DFG), grant He 3086/15-1.
29 SM participation was funded by DFG, grant ME-3534/1-2. LW, DS, IG, ME and DH are
30 grateful to the Natural Environment Research Council for funding.

Formatted: Subscript

Formatted: Subscript

Formatted: Subscript

Formatted: Subscript

Formatted: Subscript

Deleted: therefore

Formatted: Subscript

Formatted: Subscript

Formatted: Subscript

Deleted: [

Deleted:]

Moved down [2]: (Liang, J, D.J. Jacob, Effect of aqueous phase cloud chemistry on tropospheric ozone. J. Geophys. Res., 102,D5,5993-6001, 1997)

Formatted: Subscript

Formatted: Subscript

Deleted: .

Formatted: Subscript

1

2 References

3 Abbatt, J. P. D., Lee, A. K. Y., and Thornton, J. A.: Quantifying trace gas uptake to
4 tropospheric aerosol: recent advances and remaining challenges, *Chemical Society Reviews*,
5 41, 6555-6581, Doi 10.1039/C2cs35052a, 2012.

6 Bielski, B. H. J., Cabelli, D. E., Arudi, R. L., and Ross, A. B.: Reactivity of HO₂/O₂ radicals
7 in aqueous solution, *Journal of Physical and Chemical Reference Data*, 14, 1041-1100, Doi
8 10.1063/1.555739, 1985.

9 Bohn, B., Corlett, G. K., Gillmann, M., Sanghavi, S., Stange, G., Tensing, E., Vrekoussis,
10 M., Bloss, W. J., Clapp, L. J., Kortner, M., Dorn, H. P., Monks, P. S., Platt, U., Plass-Dulmer,
11 C., Mihalopoulos, N., Heard, D. E., Clemitshaw, K. C., Meixner, F. X., Prevot, A. S. H., and
12 Schmitt, R.: Photolysis frequency measurement techniques: results of a comparison within
13 the ACCENT project, *Atmos. Chem. Phys.*, 8, 5373-5391, 2008.

14 [Bohn, B.: Interactive comment, Atmos Chem Phys Discuss, 14, C7390-C7394, 2014.](#)

15 [Brauer, P., Mouchel-Vallon, C., Tilgner, A., Mutzel, A., Böge, O., Rodigast, M., Poulain, L.,
16 van Pinxteren, D., Wolke, R., Aumont, B., and Herrmann, H.: Development of a protocol
17 designed for the self-generation of explicit aqueous phase oxidation schemes of organic
18 compounds, in preparation for Atmos Chem Phys Discuss,](#)

19 Carslaw, N., Jacobs, P. J., and Pilling, M. J.: Modeling OH, HO₂, and RO₂ radicals in the
20 marine boundary layer 2. Mechanism reduction and uncertainty analysis, *Journal of
21 Geophysical Research-Atmospheres*, 104, 30257-30273, Doi 10.1029/1999jd900782, 1999.

22 Commane, R., Floquet, C. F. A., Ingham, T., Stone, D., Evans, M. J., and Heard, D. E.:
23 Observations of OH and HO₂ radicals over West Africa, *Atmos Chem Phys*, 10, 8783-8801,
24 DOI 10.5194/acp-10-8783-2010, 2010.

25 Emmerson, K. M., Carslaw, N., Carslaw, D. C., Lee, J. D., McFiggans, G., Bloss, W. J.,
26 Gravesstock, T., Heard, D. E., Hopkins, J., Ingham, T., Pilling, M. J., Smith, S. C., Jacob, M.,
27 and Monks, P. S.: Free radical modelling studies during the UK TORCH campaign in
28 summer 2003, *Atmos Chem Phys*, 7, 167-181, 2007.

29 Fuchs, H., Bohn, B., Hofzumahaus, A., Holland, F., Lu, K. D., Nehr, S., Rohrer, F., and
30 Wahner, A.: Detection of HO₂ by laser-induced fluorescence: Calibration and interferences
31 from RO₂ radicals, *Atmospheric Measurement Techniques*, 4, 1209-1225, DOI 10.5194/amt-
32 4-1209-2011, 2011.

Formatted: Font: (Default) Times New Roman, 12 pt

Deleted: Brauer, P., Tilgner, A., Wolke, R., and Herrmann, H.: Mechanism development and modelling of tropospheric multiphase halogen chemistry: The CAPRAM Halogen Module 2.0 (HM2). *Journal of Atmospheric Chemistry*, 70, 19-52, DOI 10.1007/s10874-013-9249-6, 2013.

1 George, I. J., Matthews, P. S. J., Whalley, L. K., Brooks, B., Goddard, A., Romero, M. T. B.,
2 and Heard, D. E.: Measurements of uptake coefficients for heterogeneous loss of HO₂ onto
3 submicron inorganic salt aerosols, *Physical Chemistry Chemical Physics*, 15, 12859-12845,
4 2013.

5 Haggerstone, A. L., Carpenter, L. J., Carslaw, N., and McFiggans, G.: Improved model
6 predictions of HO₂ with gas to particle mass transfer rates calculated using aerosol number
7 size distributions, *Journal of Geophysical Research-Atmospheres*, 110, Artn D04304 Doi
8 10.1029/2004jd005282, 2005.

9 Hanson, D. R., Burkholder, J. B., Howard, C. J., and Ravishankara, A. R.: Measurement of
10 OH and HO₂ Radical Uptake Coefficients on Water and Sulfuric-Acid Surfaces, *Journal of*
11 *Physical Chemistry*, 96, 4979-4985, Doi 10.1021/J100191a046, 1992.

12 Herrmann, H., Wolke, R., Muller, K., Brüggemann, E., Gnauk, T., Barzagli, P., Mertes, S.,
13 Lehmann, K., Massling, A., Birmili, W., Wiedensohler, A., Wierprecht, W., Acker, K.,
14 Jaeschke, W., Kramberger, H., Svrčina, B., Bachmann, K., Collett, J. L., Galgon, D.,
15 Schwirn, K., Nowak, A., van Pinxteren, D., Plewka, A., Chemnitz, R., Rud, C., Hofmann,
16 D., Tilgner, A., Diehl, K., Heinold, B., Hinneburg, D., Knoth, O., Sehili, A. M., Simmel, M.,
17 Wurzler, S., Majdik, Z., Mauersberger, G., and Müller, F.: FEBUKO and MODMEP: Field
18 measurements and modelling of aerosol and cloud multiphase processes, *Atmos Environ*, 39,
19 4169-4183, DOI 10.1016/j.atmosenv.2005.02.004, 2005.

20 Huijnen, V., Williams, J. E., and Flemming, J.: Modeling global impacts of heterogeneous
21 loss of HO₂ on cloud droplets, ice particles and aerosols, *Atmospheric Chemistry and Physics*
22 *Discussions*, 14, 8575-8632, 2014.

23 Jacob, D. J.: Chemistry of OH in remote clouds and its role in the production of formic acid
24 and peroxymonosulfate, *Journal of Geophysical Research-Atmospheres*, D9, 9807-9826,
25 1986.

26 Jacob, D. J.: Heterogeneous chemistry and tropospheric ozone, *Atmos Environ*, 34, 2131-
27 2159, Doi 10.1016/S1352-2310(99)00462-8, 2000.

28 Lelieveld, J., and Crutzen, P. J.: Influences of cloud photochemical processes on tropospheric
29 ozone, *Nature*, 343, 227-233, Doi 10.1038/343227a0, 1990.

30 Liang, J., and Jacob, D. J.: Effect of aqueous phase cloud chemistry on tropospheric ozone,
31 *Journal of Geophysical Research-Atmospheres*, 102, D5, 5993-6001, 1997.

32 Macintyre, H. L., and Evans, M. J.: Parameterisation and impact of aerosol uptake of HO₂ on
33 a global tropospheric model, *Atmos Chem Phys*, 11, 10965-10974, DOI 10.5194/acp-11-
34 10965-2011, 2011.

Deleted: Atmospheric

Deleted: T

Moved (insertion) [2]

Deleted: (

Deleted: , D.J.

Deleted: J. Geophys. Res.,

Deleted:)

1 | Madronich, S., and Flocke, S.: [The role of solar radiation in atmospheric chemistry](#),
2 | Handbook of Environmental Chemistry, edited by: Boule, P., Springer, New York, pp. 1-26
3 | pp., 1998.
4 | Mao, J., Fan, S., Jacob, D. J., and Travis, K. R.: Radical loss in the atmosphere from Cu-Fe
5 | redox coupling in aerosols, Atmos Chem Phys, 13, 509-519, DOI 10.5194/acp-13-509-2013,
6 | 2013.
7 | [Martin, R. V., Jacob, D. J., Yantosca, R. M., Chin, M., and Ginoux, P.: Global and regional
8 | decreases in tropospheric oxidants from photochemical effects of aerosols. Journal of
9 | Geophysical Research-Atmospheres, 108, D3, 4097, doi:10.1029/2002JD0022622, 2003.](#)
10 | Mauldin, R. L., Madronich, S., Flocke, S. J., Eisele, F. L., Frost, G. J., and Prevot, A. S. H.:
11 | New insights on OH: Measurements around and in clouds, Geophysical Research Letters, 24,
12 | 3033-3036, 10.1029/97gl02983, 1997.
13 | Mauldin, R. L., Frost, G. J., Chen, G., Tanner, D. J., Prevot, A. S. H., Davis, D. D., and
14 | Eisele, F. L.: OH measurements during the first Aerosol Characterization Experiment (ACE
15 | 1): Observations and model comparisons, Journal of Geophysical Research-Atmospheres,
16 | 103, 16713-16729, Doi 10.1029/98jd00882, 1998.
17 | Nimmo, M., and Fones, G. R.: The potential pool of Co, Ni, Cu, Pb and Cd organic
18 | complexing ligands in coastal and urban rain waters, Atmos Environ, 31, 693-702, Doi
19 | 10.1016/S1352-2310(96)00243-9, 1997.
20 | Olson, J. R., Crawford, J. H., Chen, G., Fried, A., Evans, M. J., Jordan, C. E., Sandholm, S.
21 | T., Davis, D. D., Anderson, B. E., Avery, M. A., Barrick, J. D., Blake, D. R., Brune, W. H.,
22 | Eisele, F. L., Flocke, F., Harder, H., Jacob, D. J., Kondo, Y., Lefer, B. L., Martinez, M.,
23 | Mauldin, R. L., Sachse, G. W., Shetter, R. E., Singh, H. B., Talbot, R. W., and Tan, D.:
24 | Testing fast photochemical theory during TRACE-P based on measurements of OH, HO₂,
25 | and CH₂O, Journal of Geophysical Research-Atmospheres, 109, Artn D15s10 Doi
26 | 10.1029/2003jd004278, 2004.
27 | Saunders, S. M., Jenkin, M. E., Derwent, R. G., and Pilling, M. J.: Protocol for the
28 | development of the Master Chemical Mechanism, MCM v3 (Part A): tropospheric
29 | degradation of non-aromatic volatile organic compounds, Atmos Chem Phys, 3, 161-180,
30 | 2003.
31 | Schwartz, S. E.: Gas-phase and aqueous-phase chemistry of HO₂ in liquid water clouds,
32 | Journal of Geophysical Research-Atmospheres, 89, 1589-1598, Doi
33 | 10.1029/Jd089id07p11589, 1984.

Formatted: Left, Line spacing: single,
Don't adjust space between Latin and
Asian text, Don't adjust space between
Asian text and numbers

Formatted: Font: (Default) Times New
Roman, 12 pt

1 Sehili, A. M., Wolke, R., Knoth, O., Simmel, M., Tilgner, A., and Herrmann, H.: Comparison
2 of different model approaches for the simulation of multiphase processes, *Atmos Environ*, 39,
3 4403-4417, DOI 10.1016/j.atmosenv.2005.02.039, 2005.

4 Smith, S. C., Lee, J. D., Bloss, W. J., Johnson, G. P., Ingham, T., and Heard, D. E.:
5 Concentrations of OH and HO₂ radicals during NAMBLEX: measurements and steady state
6 analysis, *Atmos Chem Phys*, 6, 1435-1453, 2006.

7 Sommariva, R., Haggerstone, A. L., Carpenter, L. J., Carslaw, N., Creasey, D. J., Heard, D.
8 E., Lee, J. D., Lewis, A. C., Pilling, M. J., and Zador, J.: OH and HO₂ chemistry in clean
9 marine air during SOAPEX-2, *Atmos Chem Phys*, 4, 839-856, 2004.

10 Spokes, L. J., Campos, M. L. A. M., and Jickells, T. D.: The role of organic matter in
11 controlling copper speciation in precipitation, *Atmos Environ*, 30, 3959-3966, Doi
12 10.1016/1352-2310(96)00125-2, 1996.

13 Taketani, F., Kanaya, Y., and Akimoto, H.: Kinetics of heterogeneous reactions of HO₂
14 radical at ambient concentration levels with (NH₄)₂SO₄ and NaCl aerosol particles, *Journal*
15 *of Physical Chemistry A*, 112, 2370-2377, Doi 10.1021/Jp0769936, 2008.

16 Thornton, J., and Abbatt, J. P. D.: Measurements of HO₂ uptake to aqueous aerosol: Mass
17 accommodation coefficients and net reactive loss, *Journal of Geophysical Research-*
18 *Atmospheres*, 110, Artn D08309 Doi 10.1029/2004jd005402, 2005.

19 Thornton, J. A., Jaegle, L., and McNeill, V. F.: Assessing known pathways for HO₂ loss in
20 aqueous atmospheric aerosols: Regional and global impacts on tropospheric oxidants, *Journal*
21 *of Geophysical Research-Atmospheres*, 113, Artn D05303 Doi 10.1029/2007jd009236, 2008.

22 Tilgner, A., Majdik, Z., Sehili, A. M., Simmel, M., Wolke, R., and Herrmann, H.:
23 SPACCIM: Simulations of the multiphase chemistry occurring in the FEBUKO hill cap cloud
24 experiments, *Atmos Environ*, 39, 4389-4401, DOI 10.1016/j.atmosenv.2005.02.028, 2005.

25 Tilgner, A., Brauer, P., Wolke, R., and Herrmann, H.: Modelling multiphase chemistry in
26 deliquescent aerosols and clouds using CAPRAM3.0i, *Journal of Atmospheric Chemistry*, 70,
27 221-256, DOI 10.1007/s10874-013-9267-4, 2013.

28 Whalley, L. K., Furneaux, K. L., Goddard, A., Lee, J. D., Mahajan, A., Oetjen, H., Read, K.
29 A., Kaaden, N., Carpenter, L. J., Lewis, A. C., Plane, J. M. C., Saltzman, E. S.,
30 Wiedensohler, A., and Heard, D. E.: The chemistry of OH and HO₂ radicals in the boundary
31 layer over the tropical Atlantic ocean, *Atmos Chem Phys*, 10, 1555-1576, DOI 10.5194/acp-
32 10-1555-2010, 2010.

33 Whalley, L. K., Blitz, M. A., Desservettaz, M., Seakins, P. W., and Heard, D. E.: Reporting
34 the sensitivity of laser-induced fluorescence instruments used for HO₂ detection to an

Deleted: Tilgner, A., Heinold, B., Nowak, A., and Herrmann, H.: Meteorological characterisation of the FEBUKO hill cap cloud experiments, part I: Synoptic characterisation of measurement periods, *Atmos Environ*, 39, 4185-4194, DOI 10.1016/j.atmosenv.2005.02.006, 2005a.¶

Deleted: b

1 interference from RO₂ radicals and introducing a novel approach that enables HO₂ and
2 certain RO₂ types to be selectively measured, Atmospheric Measurement Techniques, 6,
3 3425–3440, 2013.

4 Wolke, R., Sehili, A. M., Simmel, M., Knoth, O., Tilgner, A., and Herrmann, H.: SPACCIM:
5 A parcel model with detailed microphysics and complex multiphase chemistry, Atmos
6 Environ, 39, 4375-4388, DOI 10.1016/j.atmosenv.2005.02.038, 2005.

7

8

9

- 1 Table 1. Details of ancillary measurements used for comparison with radical observations and
 2 cubic model constraints.

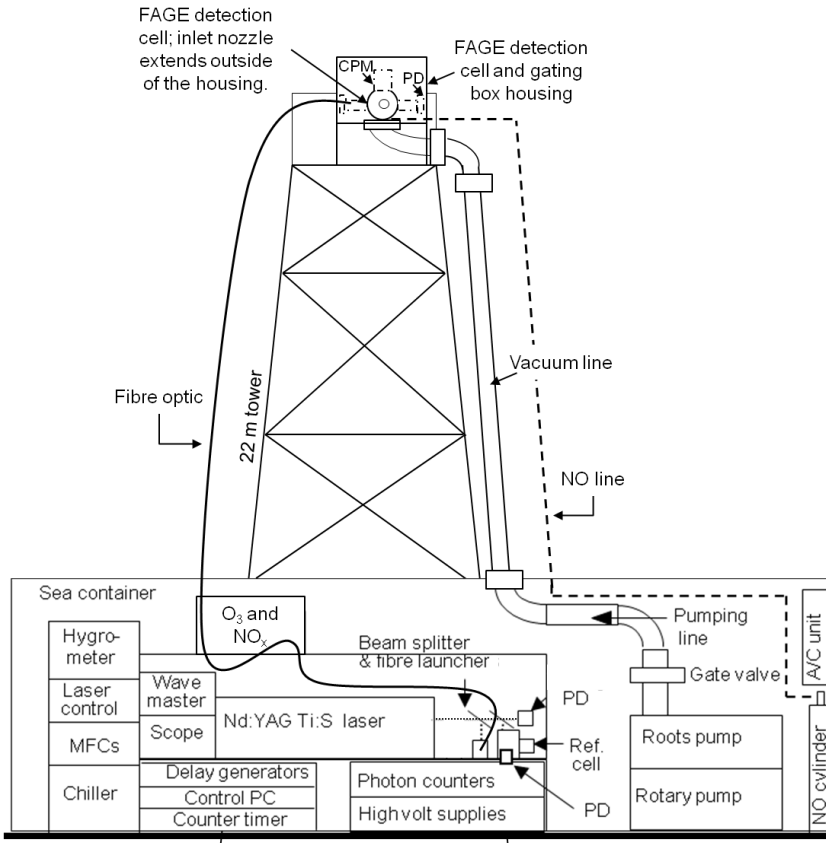
Measurement	Instrument
Liquid Water Content	Gerber particle volume monitor
Particle Surface Area (drops)	Gerber particle volume monitor
Effective Drop Radius	Gerber particle volume monitor
Temperature	Automatic weather station
Relative Humidity	Automatic weather station
$j(O^1D)$	Filter Radiometer
Cloud droplet pH	Mettler 405-60 88TE-S7/120
NO _x	Chemiluminescence detector
O ₃	TEI 42c, UV absorption
CO	Thermo Electron CO analyser
HCHO	2,4-dinitrophenylhydrazine (DNPH) cartridge samples

3

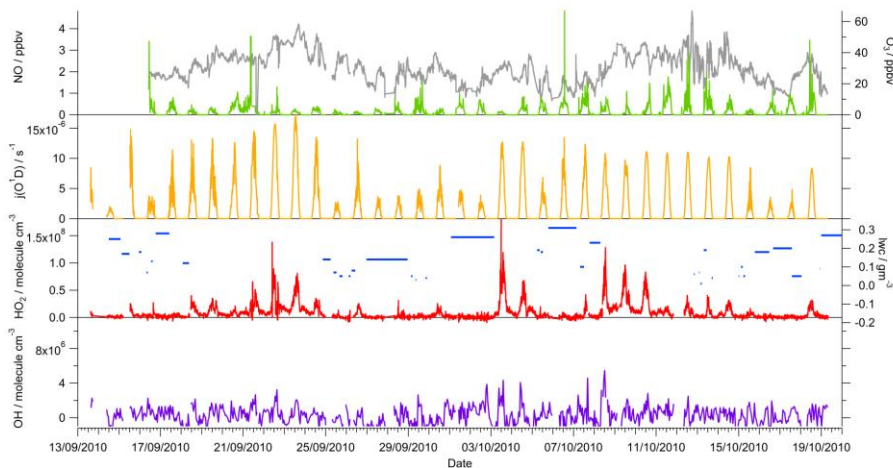
- 4 Table 2. The values used for the calculation of the theoretical uptake coefficient, black
 5 triangles, Fig. 5b, as a function of pH; values given at a pH = 5 here.

Parameter	Value	Comments
T (Temperature)	279 K	Mean HCCT-2010 temperature
H_{HO_2} (Henry's law constant)	$1.72 \times 10^4 \text{ M atm}^{-1}$	At 279 K
H_{eff} (Effective Henry's law constant)	8.8×10^4	At 279 K, pH = 5
K_{eq} (Equilibrium constant associated with R2)	$4.2 \times 10^{-5} \text{ M}$	At 279 K
k_3 (Rate constant for reaction R3)	$8.6 \times 10^5 \text{ M}^{-1} \text{ s}^{-1}$	Bielski et al.(1985)
k_4 (Rate constant for reaction R4)	$1.0 \times 10^8 \text{ M}^{-1} \text{ s}^{-1}$	Bielski et al.(1985)
k_{eff} (effective second order rate constant)	$1.65 \times 10^7 \text{ M}^{-1} \text{ s}^{-1}$	At 279 K, pH = 5
α_{HO_2} (accommodation coefficient)	1	
ω (mean molecule speed of HO ₂)	64000 cm s^{-1}	At 279 K
N_A (Avogadro's number)	$6.02 \times 10^{23} \text{ mol}^{-1}$	
R (Universal gas constant)	$0.082057 \text{ atm L mol}^{-1} \text{ K}^{-1}$	
[HO ₂]	$2 \times 10^7 \text{ molecule cm}^{-3}$	
r_p (particle radius)	6 μm	Mean cloud droplet radius

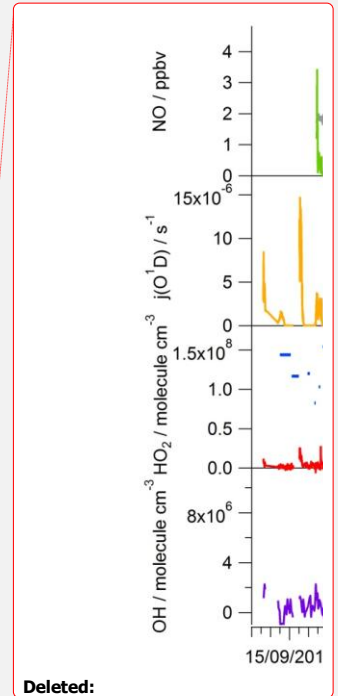
Deleted: γ_{HO_2}



1
 2 Figure 1. Schematic of the FAGE instrument setup during the HCCT-2010 campaign. 'PD'
 3 refers to photodiode, used to normalise the observed HO₂ signal to laser power.

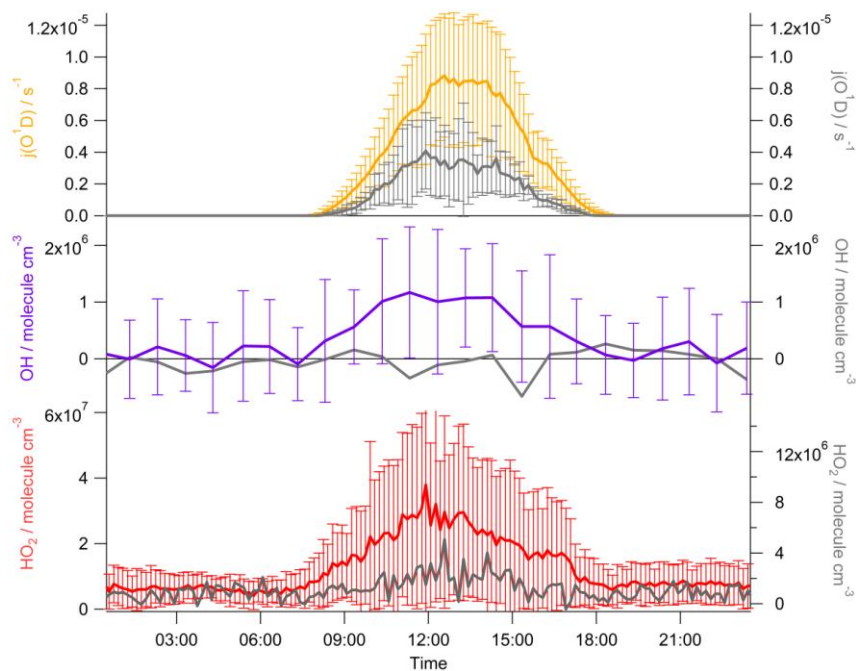


4

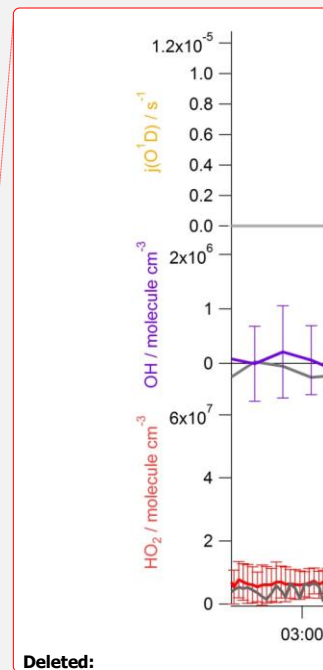


Deleted:

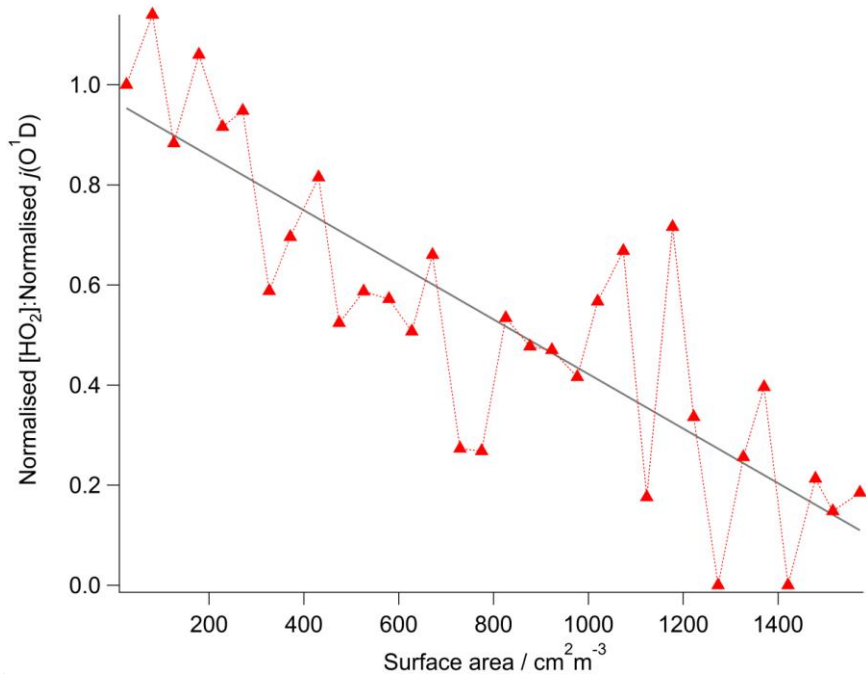
- 1 Figure 2. Time-series showing the average liquid water content during each cloud episode
- 2 (blue, horizontal lines), [OH] (purple), [HO₂] (red), j(O¹D) (orange), NO (green) and O₃
- 3 (grey). All data are the average concentrations determined for each FAGE data acquisition
- 4 cycle apart from OH concentrations which are hourly.



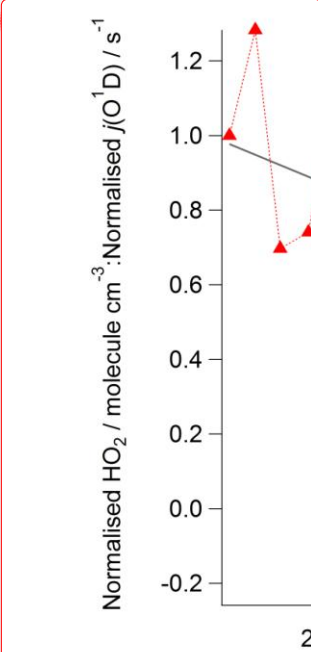
- 5
- 6 Figure 3. Average diurnal profiles of j(O¹D), OH, HO₂ in cloud (grey) and out of cloud
- 7 (coloured). The error bars represent the 1 σ variability of the averaged data; only the
- 8 variability in the out of cloud radical data is shown for clarity. Each data point represents 10
- 9 minute averaged data apart from the OH, for which the hourly averaged data are given.



Deleted:



Formatted: Font: (Default) Times New Roman, 12 pt

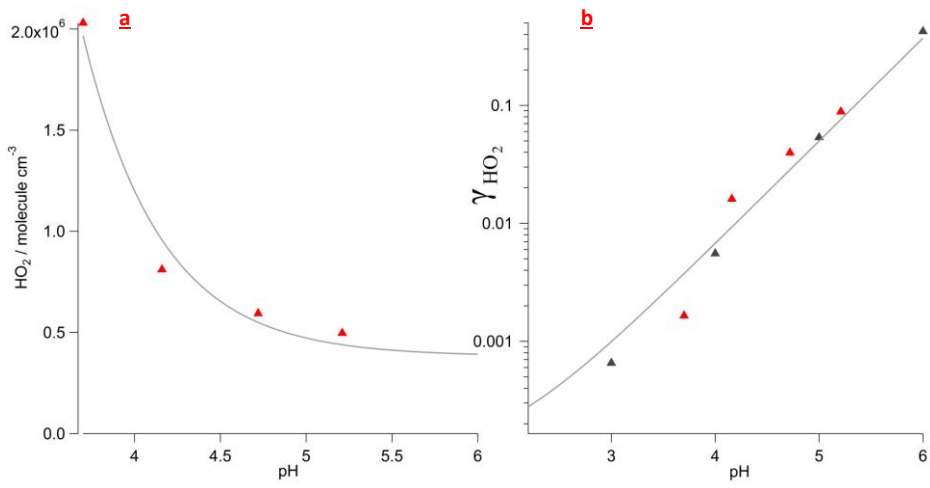


Deleted:
Formatted: Font: (Default) Times New Roman, 12 pt

1
2 Figure 4. The dependence of the measured HO₂ concentration as a function of cloud droplet
3 surface area. To remove the influence of changing photolysis rates the measured HO₂
4 concentrations have been divided by the correspondingly observed rate of photolysis of ozone
5 ($j(O^1D)$). This ratio has then been normalized to give a value of 1 when the droplet surface
6 area was zero. The systematic decrease in this normalised ratio with increasing droplet
7 surface area suggests that in addition to the reduction in HO₂ caused by a reduction in the
8 photolysis rates within clouds, there is a further loss process that increases with cloud droplet
9 surface area. The ratio decreases linearly with increasing droplet surface area up to 1500
10 $cm^2 m^{-3}$ with the line of best fit being Ratio = $1 - 5 \times 10^{-4} \times SA$.

Deleted: 6

11



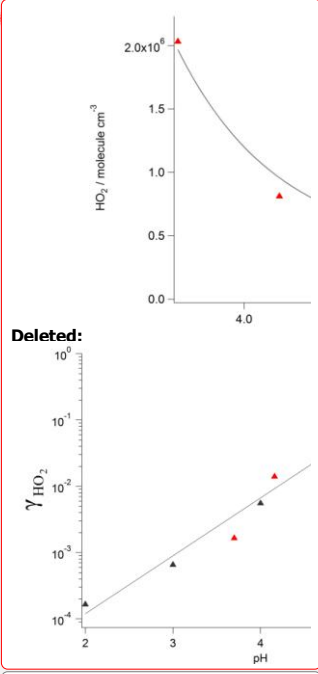
1

2 Figure 5a. Dependence of the HO₂ concentration observed in cloud as a function of cloud pH.
 3 All in-cloud HO₂ data were averaged into corresponding pH bins (0.6 pH units). The [HO₂]
 4 decreases exponentially with increasing pH with the line of best fit ($[HO_2] = 3.8 \times 10^5 +$
 5 $5.5 \times 10^9 \exp^{-2.2pH}$) displayed by the grey line. Figure 5b. The cloud uptake coefficient
 6 estimated by optimizing the HO₂ concentration calculated from the analytic expression of
 7 Carlsaw et al. (1999) compared to the observed HO₂ concentration as a function of pH (red
 8 triangles). The theoretical expression derived by Thornton et al. (2008) (Eq. (4)) using
 9 parameters provided in Table 2 is shown as the black triangles with the grey line being a best-
 10 fit line for these data ($\gamma_{HO_2} = 2.15 \times 10^{-6} \exp^{2.01pH}$).

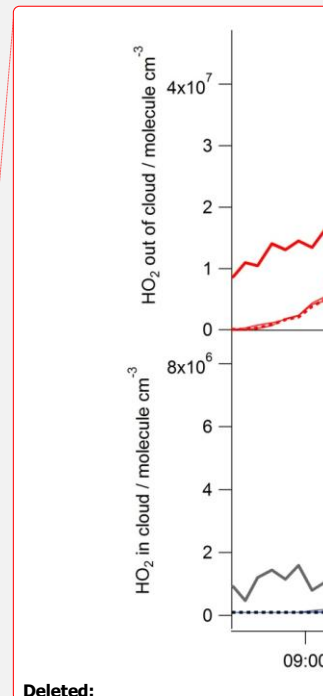
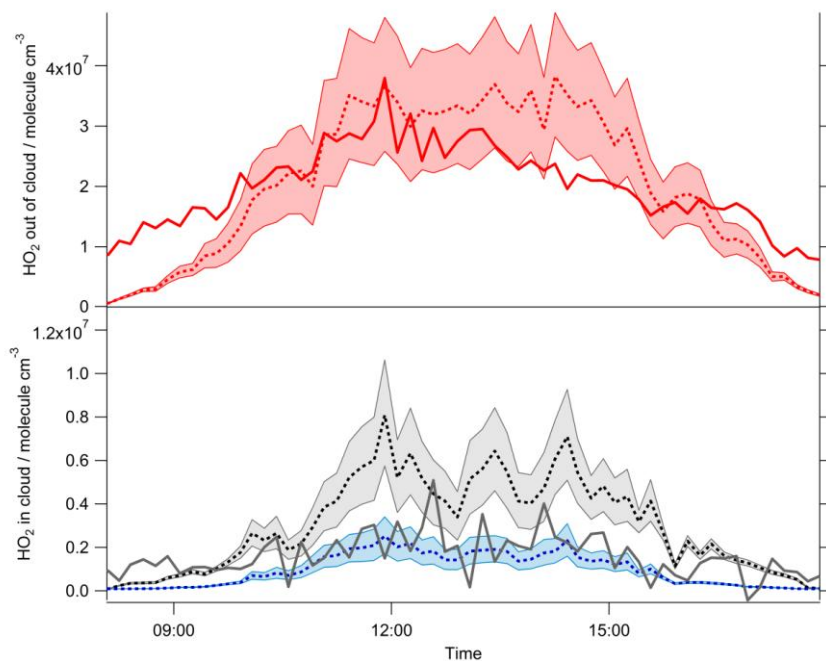
11

12

Formatted: Font: (Default) Times New Roman, 12 pt

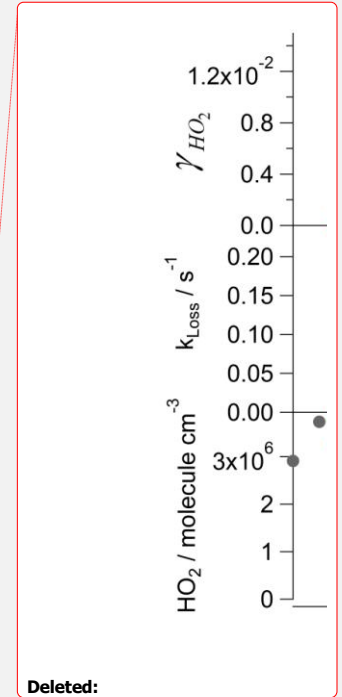
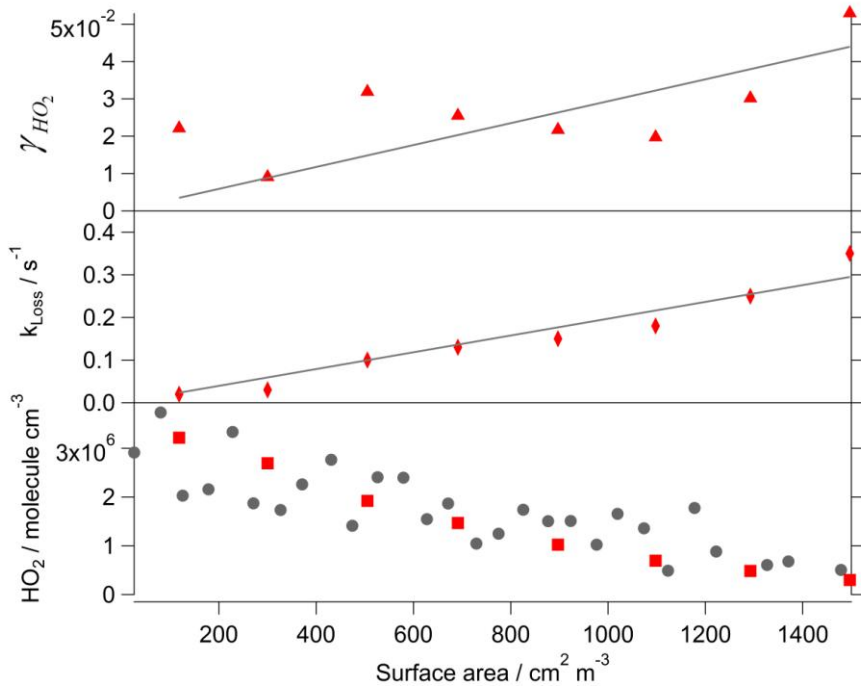


Formatted: Font: (Default) Times New Roman, 12 pt



1
 2 Figure 6, Upper panel. Average measured (solid red line) and simulated (dashed red line)
 3 diurnal profile of HO₂ concentrations outside of cloud events. The simulation is based on an
 4 expression originally determined by Carslaw et al. (1999) and described further in Sect. 2.2.
 5 The shading highlights the sensitivity of the model to $\pm 1\sigma$ changes in the CO and HCHO
 6 concentrations used as constraints.
 7 Lower panel. Average measured (solid grey line) and modelled (dashed black and blue lines)
 8 diurnal profile of HO₂ concentration during cloud events. The model was run without (grey)
 9 and with (blue) a loss of HO₂ to cloud droplets equal to a first order loss rate of 0.1 s⁻¹. The
 10 shading highlights the sensitivity of the model to $\pm 1\sigma$ changes in the CO and HCHO
 11 concentrations used as constraints.

12



Deleted:

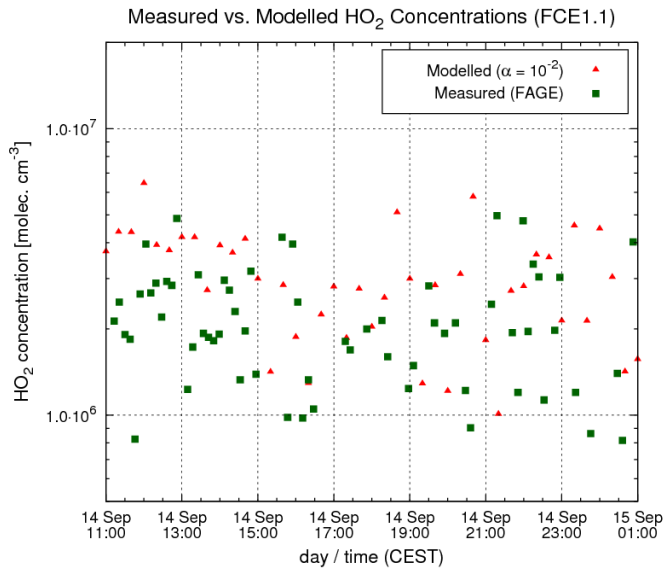
Formatted: Font: (Default) Times New Roman, 12 pt

Formatted: Font: (Default) Times New Roman, 12 pt

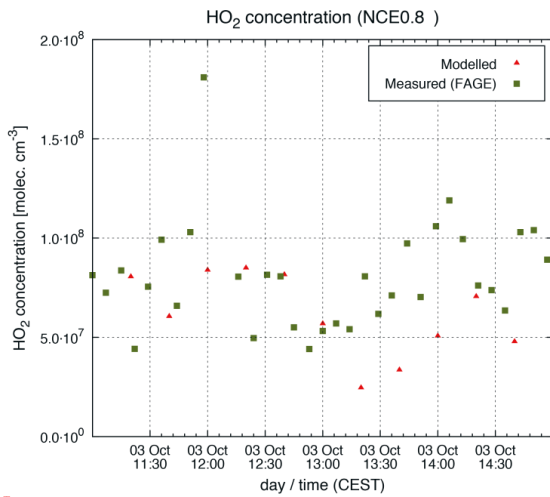
Deleted: 1

Deleted: 4

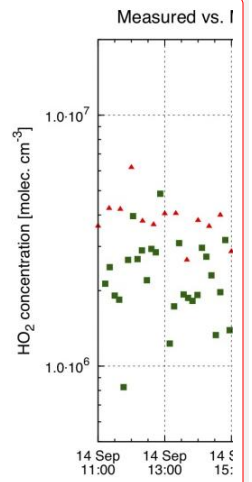
- 1
- 2 Figure 7, lower panel. The dependence of the measured HO₂ concentration (grey circles) and
- 3 modelled HO₂ concentration with a variable first order loss (red squares) as a function of
- 4 cloud droplet surface area.
- 5 Middle panel. The dependence of the first order loss term used in the model expression to
- 6 best replicate the observed in-cloud HO₂ as a function cloud droplet surface area. The line of
- 7 best fit being ($k_{Loss} = 2 \pm 0.1 \times 10^{-4} \times SA$).
- 8 Upper panel. The dependence of γ_{HO_2} calculated using Eq. 7 as a function of cloud droplet
- 9 surface area and constrained with the variable first order loss term as shown in the middle
- 10 panel. The line of best fit being ($\gamma_{HO_2} = 2.9 \pm 0.5 \times 10^{-5} \times SA$).



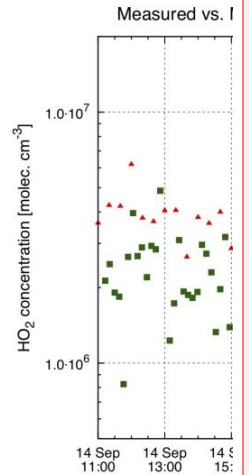
1
2 Figure 8. Comparison of the measured (green squares) and modelled (red triangles), gas
3 phase HO₂ concentrations at Mt. Schmücke site during cloud event FCE1.1 (14th, 15th Sept.
4 2010 11:00-01:00 CEST).



6

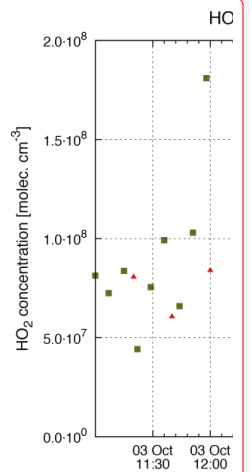


Deleted:



Deleted:

Deleted: ¶



Deleted:

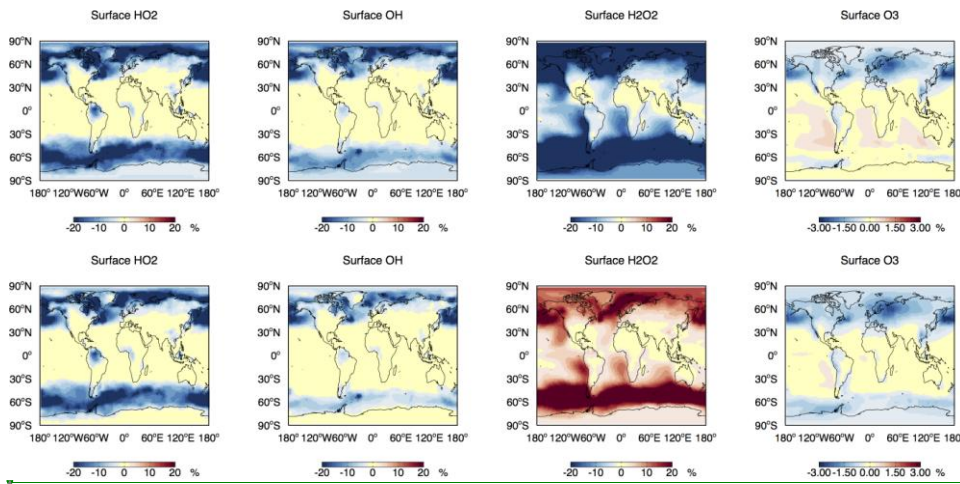
Formatted

...

1 Figure 9. Comparison of the measured (green squares) and modelled (red triangles) gas phase
 2 HO₂ concentrations at Mt. Schmücke site during the non-cloud event NCE0.8.

3

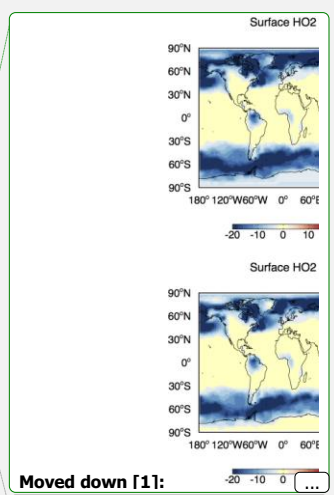
4



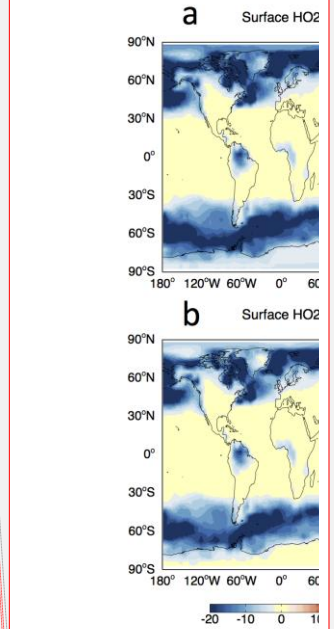
5

6 Figure 10. Annually average fractional change in surface HO₂, OH, H₂O₂ and O₃ with the
 7 inclusion of HO₂ uptake into clouds leading to a) the production of H₂O and b) the production
 8 of H₂O₂ assuming a cloud pH of 5 and the Thornton et al. (2008) parameterization.

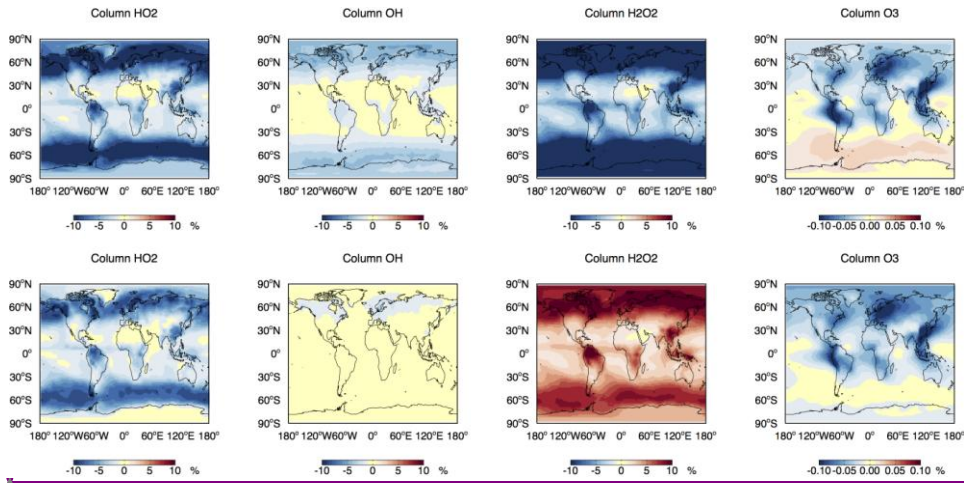
9



Moved down [1]:
 Formatted: Font: (Default) Times New Roman, 12 pt

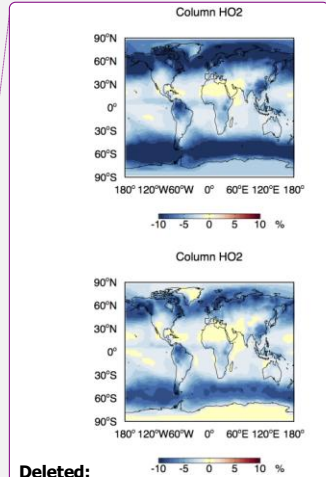


Deleted:
 Formatted: Font: (Default) Times New Roman, 12 pt
 Deleted: H₂O₂
 Formatted: Font: +Body, 11 pt
 Moved (insertion) [1]
 Formatted: Font: (Default) Times New Roman, 12 pt
 Deleted: Page Break
 Formatted: Font: 12 pt
 Deleted: 11... Annually
 Formatted: Not Superscript/ Subscript
 Field Code Changed
 Formatted: Font: +Body, 11 pt



1
2 Figure 11. Annually averaged fractional change in column HO_2 , OH , H_2O_2 and O_3 with the
3 inclusion of HO_2 uptake into clouds leading to a) the production of H_2O and b) the production
4 of H_2O_2 assuming a cloud pH of 5 and the Thornton et al. (2008) parameterization.

5

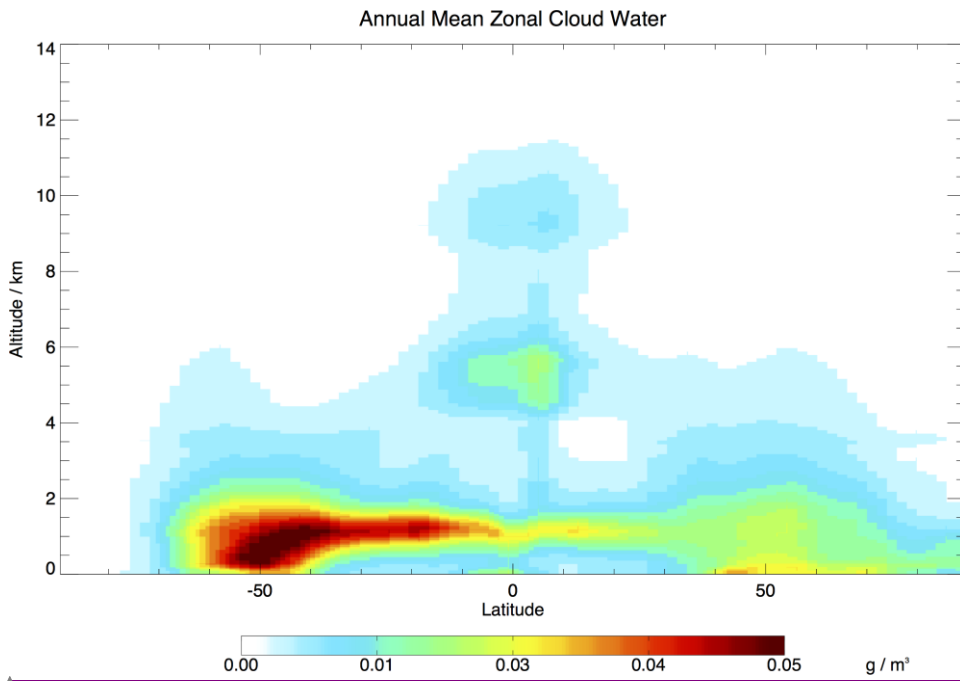


Deleted:
Figure 11. Annually averaged fractional change in column HO_2 , OH and H_2O_2 with the inclusion of HO_2 uptake into clouds leading to a) the production of H_2O and b) the production of H_2O_2 assuming a cloud pH of 5 and the Thornton et al. (2008) parameterization. ¶

Formatted: Font: (Default) Times New Roman, 12 pt

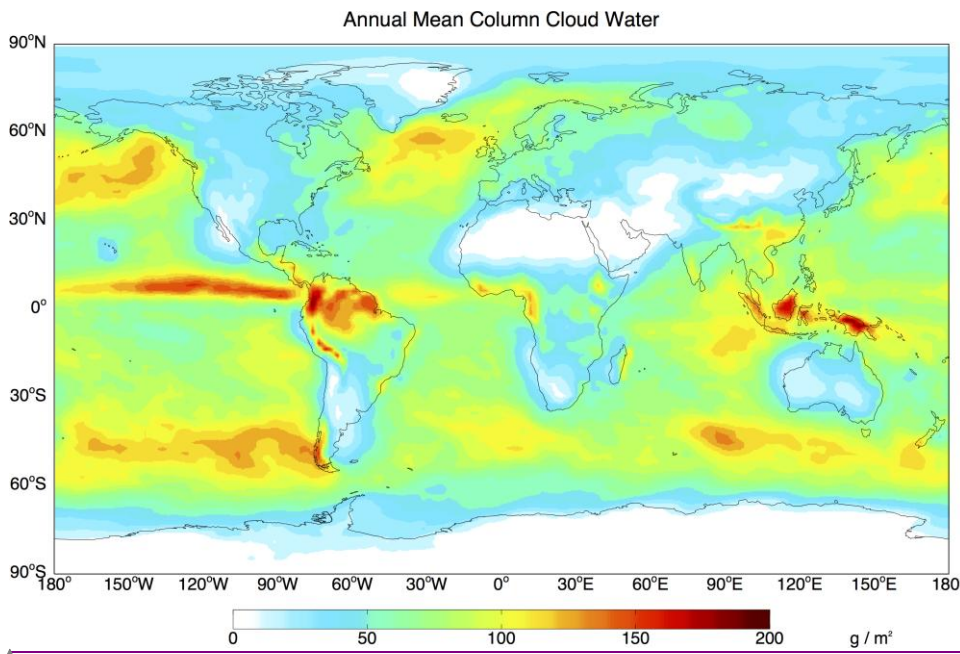
Formatted: Font: (Default) Times New Roman, 12 pt

1



Formatted: Font: (Default) Times New Roman, 12 pt, Bold, Font color: Text 1

2



Formatted: Font color: Text 1

3

1 Figure 12. Annually averaged cloud water in the GEOS5 fields as a) a column total and b) a
2 zonal mean.

Formatted: Font: (Default) Times New Roman, 12 pt

Deleted: ¶